# MECHANISTIC-EMPIRICAL APPROACH FOR THE ANALYSIS OF SUBGRADE AND GRANULAR LAYERS OF FLEXIBLE PAVEMENT USING IITPAVE AND KENPAVE

A PROJECT REPORT

Submitted by

**SHAHNA N**

**TKM20CETE13**

to

the A P J Abdul Kalam Technological University

in partial fulfilment of the requirements for the award of the Degree

of

Master of

Technology

In

*Transportation*

*Engineering*


**DEPARTMENT OF CIVIL ENGINEERING**

T.K.M. College of Engineering, Kollam

July 2022

# DECLARATION

I undersigned hereby declare that the project report “Mechanistic-empirical approach for the analysis of subgrade and granular layers of flexible pavement using IITPAVE and KENPAVE”, submitted for partial fulfillment of the requirements for the award of degree of Master of Technology of the APJ Abdul Kalam Technological University, Kerala is a bonafide work done by me under the supervision of Prof. Karthik S. This submission represents my ideas in my own words and where ideas or words of others havebeen included, I have adequately and accurately cited and referenced the original sources. I also declare that I have adhered to ethics of academic honesty and integrity and have not misrepresented or fabricated any data or idea or fact or source in my submission. I understand that any violation of the above will be a cause for disciplinary action by the institute and/or the University and can also evoke penal action from the sources which havethus not been properly cited or from whom proper permission has not been obtained. This report has not been previously formed the basis for the award of any degree, diploma or similar title of any other University.

Kollam SHAHNA.N

08-07-2022

## DEPARTMENT OF CIVIL ENGINEERING

## T.K.M. COLLEGE OF ENGINEERING, KOLLAM

# CERTIFICATE

Certified that this report entitled **'MECHANISTIC-EMPIRICAL APPROACH FOR THE ANALYSIS OF SUBGRADE AND GRANULAR LAYERS OF FLEXIBLE PAVEMENT USING IITPAVE AND KENPAVE'** is the report of thesis presented by **SHAHNA N, Roll No.: TKM20CETE13** during **2021-2022** in partial fulfillment of the requirements for the award of the Degree of Master of Technology in Transportation Engineering of the A P J Abdul Kalam Technological University.

| Guide: | Project coordinator: | Head of the Department: |
|---|---|---|
| **Prof. Karthik S.** | **Dr. Kavitha Madhu.** | **Dr. Sajeeb R.** |
| Assistant Professor | Associate Professor | Professor |
| Dept. of Civil Engg. | Dept. of Civil Engg. | Dept. of Civil Engg. |

# ACKNOWLEDGEMENT

I take this opportunity to express my deep sense of gratitude and sincere thanks to all those who had helped me to complete my project successfully.

I am deeply indebted to my guide, **Prof. Karthik S.**, Assistant Professor, Department of Civil Engineering for his excellent guidance, positive criticism and valuable comments.

I am greatly thankful to my project coordinators, **Dr. Kavitha Madhu**, Associate professor, Department of Civil Engineering, **Prof. Meenu Tomson**, Assistant Professor, Department of Civil Engineering and **Prof. Jijin A.,** Assistant Professor, Department of Civil Engineering for their constant supervision as well as for providing necessary information regarding the project.

I am greatly thankful to **Dr. Sajeeb R.**, Head of the Department of Civil Engineering, for his kind support.

Finally, I thank my parents and friends who directly and indirectly contributed to the successful completion of my project.

**SHAHNA N**

# ABSTRACT

Premature failure of pavements is a severe issue that affects many regions, though the causes can vary. The majority of design procedures assume that the subgrade is lying approximately 500 mm above the high flood level. But heavy rainfall causes a segment of the pavement, or even the entire structure to be submerged in several areas of the country. For rural roads, where pavements are built on the available land without even providing embankment, the issue is more serious. According to the results of numerous research, subgrade soil loses strength over time when it is submerged. Additionally, a drop in the subgrade's rutting life and fatigue value is seen. Also, a submerged subgrade exhibits higher damage and decreased structural strength due to a drop in the elastic moduli of the granular and subgrade layers, as well as an abrupt jump in roughness index (as determined by the International Roughness Index). In order to maintain adequate strength and resilience to support the imposed traffic load regardless of unfavourable conditions like severe rainfall and flooding, subgrade soil must have an appropriate value of CBR. The elastic moduli of the subgrade and granular layers can be enhanced by a properly stabilized subgrade, which can also provide long-term performance and improve the CBR. The use of geosynthetics and geogrids as reinforcement is one of the strategies used today to strengthen subgrade and granular layers. Using pavement design software's such as IITPAVE and KENPAVE, this study examined the effects of improving the elastic moduli of the subgrade and granular layers associated with an increase in CBR as well as the effect of varying the thickness of the pavement layers over various mechanistic empirical parameters. Through damage analysis in KENPAVE, the study also evaluates the extent of pavement damage. The analysis shows that, the damage associated with the pavement structures for modified cases are reduced by about 45%, from the conventional cases, and hence design was modified. The effect of variation on the pavement performance parameters due to the change in bituminous course and Granular base and subbase course thicknesses by ±25%, designed for improved material properties and effective CBR, was also examined and from the results, an increase in fatigue and rutting lives was observed for even thin-bituminous surfaced pavements. A suitable cost-efficient pavement section was chosen with reference to DSR, 2021. The study also attempts to design a geogrid-reinforced pavement section for a further reduced thickness of granular layers.

**Keywords:** *Subgrade, Modulus of resilience, California Bearing Ratio (CBR), Rutting, fatigue, Geosynthetics, Geogrids, IITPAVE, KENPAVE.*

# TABLE OF CONTENTS

# LIST OF FIGURES

# LIST OF TABLES

# ABBREVIATIONS

| | |
|---|---|
| IRC | Indian Road Congress |
| HDM | Highway Development and Management |
| AASHTO | American Association of State Highway and Transportation Officials |
| ASTM | American Society for Testing and Materials |
| BIS | Bureau of Indian Standards |
| MEPDG | Mechanistic- Empirical Pavement Design Guide |
| FWD | Falling Weight Deflectometer |
| HMA | Hot Mix Asphalt |
| RD | Road- Deterioration |
| OMC | Optimum Moisture Content |
| MDD | Maximum Dry Density |
| CBR | California Bearing Ratio |
| IRI | International Roughness Index |
| $M_{RS}$ | Modulus of Resilience of subgrade |
| $M_{RGRAN}$ | Modulus of resilience of granular layer |
| $w_L$ | Liquid limit |
| $w_P$ | Plastic limit |
| $I_P$ | Plasticity Index |
| ISC | Indian Standard Classification System |
| USC | Unified Soil Classification System |
| GI | Group Index |
| Cu | Uniformity coefficient |
| Cc | Coefficient of curvature |
| DSR | Delhi Schedule of Rates |
| GSB | Granular Sub Base |
| WMM | Wet Mix Macadam |
| DBM | Dense Bituminous Macadam |

# CHAPTER 1

# INTRODUCTION

## 1.1 GENERAL

Flexible Pavements are made of bituminous or unbound material, and the lateral distribution of the applied load with depth transmits the stress to the sub-grade. Although some "full depth" asphalt surfaces are constructed directly on the subgrade, the majority of asphalt surfaces are constructed over a gravel basis. Three purposes are served by flexible pavements, and each of these requires a number of layers to be effective. The primary (visible) purpose is to create a surface that is secure, slick, and long-lasting enough to withstand the projected traffic during the course of the design. The second crucial role is to evenly distribute the loads from the vehicle tyres onto the subgrade so that it does not deform with repeated loading. Finally, it's critical to prevent water from having any negative effects on the subgrade and lower pavement layers. A flexible pavement really has five or six layers, separated into the foundation section and the pavement section, which overlap (figure 1.1).

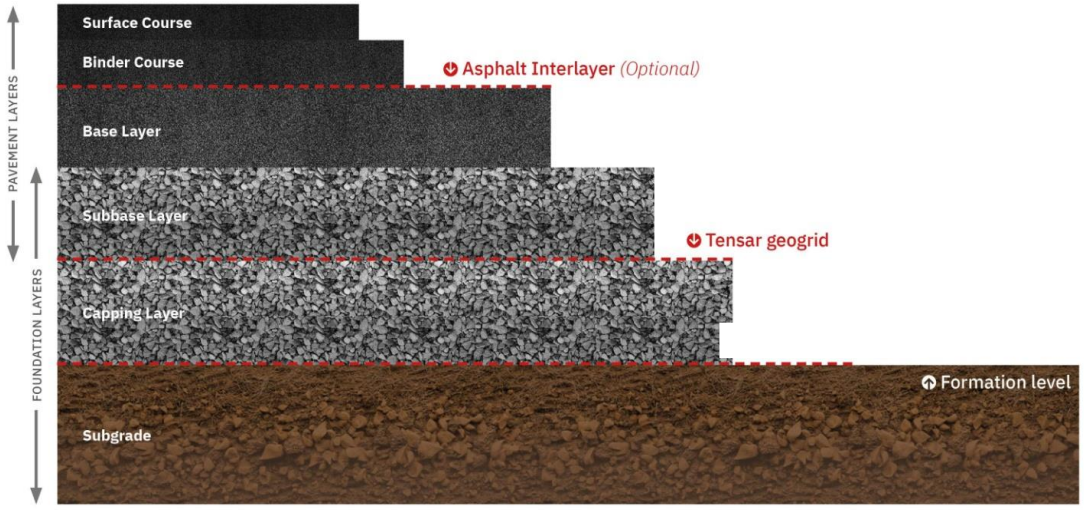


Figure 1.1 Layers of flexible pavement (Source: Introduction to pavement design, Civil IITB)

Highways serve to provide a public route for travellers in conditions of reasonable comfort. There are several approaches used for flexible pavement design by referring to standard theoretical basis, one of them is mechanistic empirical method. Flexible pavement design is

influenced by various environmental conditions at each location or region. Multilayer elastic theory is used to establish critical pavement reactions like stresses and strains, which are then connected with pavement field performance using empirical models. The loading on the road infrastructure increases over time, both in terms of traffic volume and vehicle axle load. Surprisingly, tyre pressure can have a significant impact on rutting, pavement fatigue, and stresses and strains in the higher portions of pavement structures. As a result, both from a capacity and bearing strength perspective, the road needs to be able to sustain properly. When a road's infrastructure is damaged due to being unable to support the weight of passing vehicles, the stress and strain on the road reaches a catastrophic level. Researchers are increasingly using 3D-FEM: three-dimensional finite element software to analyse pavements as high-performance computers have developed, in an effort to better understand how pavements respond to traffic and environmental loadings. The finite element approach is a computational method for analysing stresses and displacements in structures that divides a simulated structure into elements and connects them using nodes. Finite element analysis software is split into two categories: generic finite element software, like ANSYS and ABAQUS, which analyse any structure, and specialised finite element software for pavement analysis. The correctness of the results depends on the amount, type, and arrangement of the elements. KENSLAB, FEACONS, WESLAYER, LLISLAB, and JSLAB are examples of finite element programmes using the classical thin plate theory, whereas EverFE is a three-dimensional finite element analysis programme that was initially developed by the universities of Washington and Maine to simulate the responses of jointed plain rigid pavement subjected to various traffic loads and temperature gradients. As opposed to commercial software like AASHTOW, PAVERS, Win PAS 12, Street Pave, MXROAD Suite, and Infra Works software, free software for flexible pavement includes IITPAVE, KENPAVE, Pave Xpress, PAKPAVE, MICH PAVE, and ILLIPAVE.

## 1.2 PROBLEM STATEMENT

The surface course, one of the three layers in traditional flexible pavements, is intended to improve riding comfort, imperviousness, friction, and visibility. The sub-base layer serves as a drainage medium when the base course serves as a load-distribution layer. The sub-grade serves as the base, taking on all of the weight that is transmitted from the wheels through the component layers. Flexible pavements with poor design suffer distresses sooner than those

with good design. Although distress is a crucial part of pavement design, construction, material qualities, and maintenance flaws are often to blame for structural distresses. Rutting, which initially develops quickly and then slows down to a much slower rate throughout the first several years, is a characteristic pattern of structural failure in flexible pavements. It takes a lot of loading before fatigue or alligator cracking develops, and once it occurs, it gets worse and weakens the pavement. Pavements that typically deteriorate and spall under traffic develop transverse and longitudinal cracking as a result of climate fluctuations. In recent years, persistent deformation (rutting) on roadways has become more severe and extensive, particularly as a result of subpar subgrades. Greater axle weights, increased traffic, and poor subgrade are all causes of the increased rutting. Rutting is a condition that worsens with more load applications and is brought on by a combination of shear-related deformation and densification, which can happen in any layer of the pavement structure. Two different types of rutting exist. In one kind, repeated loads depress the pavement into a weak underlayment and a weak subgrade, subbase, or base course beneath the surface layer permits permanent strain to develop. This kind of rutting is typically more linked to the underlying materials and pavement structural design than it is to the surface materials. The other kind of rutting is brought on by surface wear or paving mix instability, which causes material to flow onto both sides of the wheel path. The amount of loads and relative strength of the pavement layer dictate the layer in which rutting takes place. Pavement premature failure is a severe issue that affects many nations, even though the causes can vary. The majority of design procedures assume that the subgrade is lying approximately 500 mm above the high flood level. But heavy rainfall causes a segment of the pavement, or even the entire structure, to be submerged in several areas of the country. For rural roads, where pavements are built on the available land without an embankment, the issue is more serious. One such condition of rural roads in Kainakary, Alappuzha is shown in Figures 1.2 and 1.3 Heavy rainfall is one type of extreme weather, which increases the risk of flooding on several subtropical and tropical routes. However, little study has been done to calculate these losses and create potential countermeasures.

Figure 1.2 Condition of a rural road in Kainakary, Alappuzha

Figure 1.3 Condition of a road adjacent to the A-C road section which was under submergence in Kainakary, Alappuzha during the 2018 Kerala floods
(Source: www.onmanorama.com)

The Resilient Modulus ($M_R$) of the pavement layers is a significant factor, and the Indian Roads Congress (IRC) provides pavement design sections for various circumstances. Unbound layers like base, subbase, and subgrade are crucial to how well pavements work structurally. The stiffness of these materials can be drastically decreased by an increase in moisture content. When pavement layers are exposed for an extended period of time to an excessive moisture content, it can severely reduce their ability to support traffic, degrade the integrity of the materials, and cause significant permanent deformation. The international

roughness index often reveals a sharp increase in the roughness index of a flood-affected pavement and decreased structural strength due to a drop in the resilient modulus of the granular and subgrade layers. Because of this, the pavement reacts poorly and degrades more quickly after a flood. Pavement thickness and drainage systems must be properly planned, and post-flood traffic control may need to be implemented, in order to lessen the negative consequences of flooding. On the other hand, the components in each layer of the road pavement get saturated when the roads are submerged for an extended period of time. When subgrade soil is submerged for a longer period of time, its strength decreases even more (Ghani et al. 2016, Elshaer et al. 2017, Wang et al. 2014). To maintain sufficient strength and resilience to handle the imposed traffic load regardless of unfavourable conditions such severe rainfall and flooding, subgrade soil must have an appropriate value of CBR. However, some subgrade soils have significantly low and, as a result, incorrect CBR values, making them unable to meet this criterion. Geosynthetic reinforcement technique is one of the strategies used nowadays to stabilise the subgrade and granular layers. Geosynthetics include geotextiles and geogrids. These geosynthetics serve as granular materials as well as reinforcement for the soil. They also perform additional tasks such drainage, sealing, filtration, and separation. A well stabilised subgrade can perform over time, increase CBR, and therefore increase soil $M_R$. In order to maintain proper drainage, strength, and to prevent a loss of resilience, studies demonstrating the requirement for providing adequate materials in subgrades and granular layers of pavements in flood-prone locations must be done. Through layer stabilisation and/or strengthening overlay, a pavement's tensile strength may be increased. A road may also become a stiff or composite pavement by stabilising the granular layers. In addition to using materials resistant to moisture, good drainage and load restrictions during the flood period would also assist prevent road damage.

## 1.3 STRESSES IN FLEXIBLE PAVEMENTS

Huang (2004) thought of a flexible pavement as a homogeneous half-space to describe how it would behave when subjected to wheel loads. A half-space has an infinitely deep bottom and an infinitely large top, and the loads are applied to the top plane. The foundation of the original Boussinesq theory was a focused load applied to an elastic half space. To determine the reactions due to loading over a circular region, the stresses, strains, and deflections in a pavement structure due to a concentrated load can be integrated. Based on the behaviour of

the pavement materials utilised, several hypotheses are available for the understanding of these responses in a flexible pavement. However, no one theory is likely to fully account for all features in the design and study of flexible pavements due to the numerous and complicated factors involved. Although it is not entirely accurate in the case of wheel loads applied through pneumatic tyres, the stresses in flexible pavements are typically calculated using three-layer concepts and the assumption that a uniformly distributed load is applied over a circular contact area. Considering layer system generally the analytical solution to the state of stress or strain has several assumptions as listed below:

- The material properties of each layer are homogeneous
- Each layer has a finite thickness except for the lower layer, and all are infinite in the lateral directions
- Each layer is isotropic, i.e., the property at a specific point is the same in every direction
- Full friction is developed between layers at each interface
- Surface shear forces are not present at the surface
- The stress solutions are characterized by the material properties for each layer, poisson's ratio and elastic modulus.

The critical stresses that can be calculated using three-layer systems include, σz1: Vertical stress at interface 1; σz2: Vertical stress at interface 2σr1: Horizontal stress at the bottom layer 1; σr2: Horizontal stress at the bottom layer. Figure 1.4 shows a three-layered pavement system, having surface, base and sub- grade as the three layers. h1, E1, μ1 are the depth, modulus of elasticity and Poisson's ratio of surface course. h2, E2, μ2 and h3, E3, μ3 are the corresponding values of base course and sub-grade respectively. The sub-grade is considered to be of infinite thickness. P is the load applied, while p is the tyre pressure. Figure 1.5 illustrates the critical failure points in the flexible pavements. The vertical stress on the top of subgrade is an important factor in pavement design. The function of a pavement is to reduce the vertical stress on the subgrade so that detrimental pavement deformations will not occur. The allowable vertical stress on a given subgrade depends on the strength or modulus of the subgrade. To combine the effect of stress and strength, the vertical compressive strain has been used most frequently as a design criterion. The stresses in a two-layer system depend on the modulus ratio E1/E2 and the thickness radius ratio h1/a.

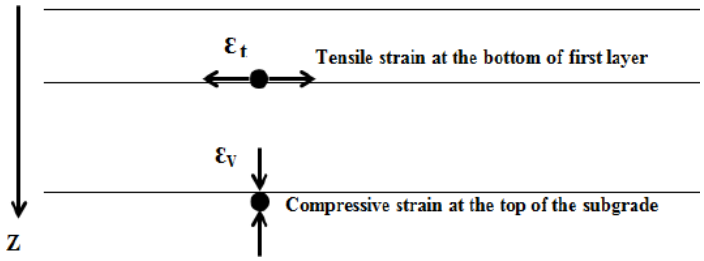


Figure 1.4 Three-layer system (Source: Lekha, 2016)

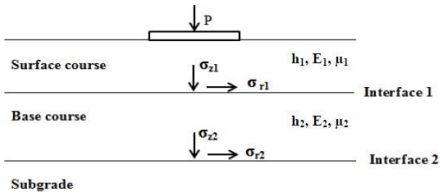


Figure 1.5 Failure modes and Critical strains for flexible pavement (Source: Lekha, 2016)

## 1.4 KENPAVE SOFTWARE

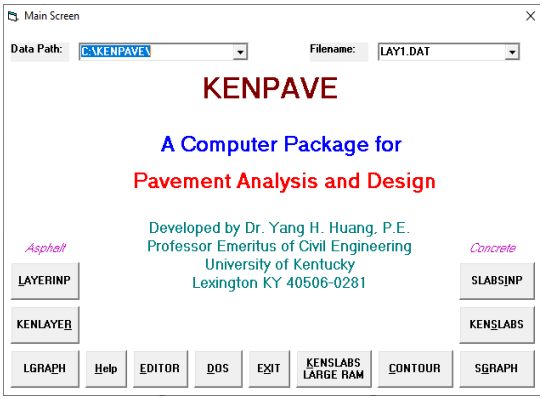


Figure 1.6 Main screen of KENPAVE

The second edition of Huang's book "Pavement Analysis and Design" is packed with the KENLAYER programme, which was created at the University of Kentucky in the United States. The application is a component of the KENPAVE software suite, together with its data input interface LAYERINP and graphic programme LGRAPH. It also contains

KENSLABS, a comparable application used for rigid pavement analysis. The software can analyse pavements with up to 19 layers and output results (strains, deflections, and stresses) in 10 different radial coordinates or 19 different vertical coordinates. Utilizing superposition and the x and y coordinate system of referencing, consideration is also given to tandem and tridem wheel configurations. Based on a fourth order differential equation, layered systems are generalised for the purpose of solving stresses, strains, and deflections in the KENLAYER programme (Omer et al., 2018). The primary screen of the KENPAVE software is depicted in Figure 1.6.

## 1.5 IITPAVE SOFTWARE

IITPAVE Software is a mechanistic-empirical software used for the design, analysis of the flexible or bitumen pavement. The input data used in this program to obtain stresses and strains at different layers are the elastic modulus, Poisson's ratio, the thickness of different layers, wheel load and tyre pressure of a vehicle. The result of strains obtained from IITPAVE software will be compared with the allowable strains and if the strains obtained are less than the allowable standard strains then the pavement thickness is called satisfied.


Figure 1.7 Main screen of IITPAVE

## 1.6 OBJECTIVES AND SCOPE OF THE STUDY

The objectives of the proposed study are as follows:

- To classify the soil samples collected from the respective locations and check for its suitability as a subgrade material.
- To study the effect of variation of thicknesses and elastic moduli of pavement layers and subgrade, on the various mechanistic parameters and thereby analyze the extent of damage of flexible pavement
- To study the effect of submergence of the subgrade layer on various mechanistic parameters.
- To choose cost-efficient and reduced pavement sections designed for improved elastic moduli and effective CBR, which are suitable from the various combinations of pavement layer thicknesses.
- To design a further reduced pavement section using geogrid-reinforcement.

The scope of the study includes the analysis of the responses from the pavement design softwares like KENPAVE and IITPAVE and the design of flexible pavement using these critical parameters under dual wheel condition. . In this study, the effect of improvement of elastic moduli of pavement layers associated with an increase in CBR and the effect of variation of thickness of pavement layers over various mechanistic empirical parameters was studied. The study also analyses the extent of damage of pavement through damage analysis. The effect of variation in bituminous course and Granular base and subbase course thicknesses by ±25%, designed for improved elastic properties and effective CBR, on the pavement performance parameters was also examined. The study also attempts to design a geogrid-reinforced pavement section for a further reduced thickness of granular layers. However, the part of the study focusing on the effect of variation of mechanistic parameters over the period of submergence is limited only to the subgrade layer of the pavement. The geotextiles provided in the subgrade layer and geogrids provided in the granular layers are placed as single-layer reinforcement.

# CHAPTER 2

# LITERATURE REVIEW

## 2.1 GENERAL

Hankare et al. (2018) projected that a lower $M_R$ & CBR and subsequently a shorter pavement life caused an increase in pavement deflection at Kolhapur to Teraswadi Road in the Maharashtra area. They have collected all information regarding pavement as follows:

- CBR (California Bearing Ratio) Value [CBR value before and after flooding was collected from PWD office as shown in tables 2.1 and 2.2]
- $M_R$ (Modulus of Resilience) Value [obtained from CBR value using equations provided as per IRC 37, 2018]
- Rutting life [Rutting model, IRC 37, 2018]
- Fatigue life [Fatigue model, IRC 37, 2018]

Table 2.1 CBR before flooding (Source: Hankare et al., 2018)

| **Penetration (mm)** | **Load(kg)** | | |
|---|---|---|---|
| | Average | Trial 1 | Trial 2 |
| 0.5 | 20 | 22 | 18 |
| 1 | 40 | 41 | 39 |
| 1.5 | 55 | 56.5 | 53.5 |
| 2 | 70 | 73 | 67 |
| 2.5 | 80 | 81 | 79 |
| 3 | 100 | 100.5 | 99.5 |
| 4 | 115 | 117 | 113 |
| 5 | 120 | 122 | 118 |

Table 2.2 CBR after flooding (Source: Hankare et al., 2018)

| **Penetration (mm)** | **Load(kg)** | | |
|---|---|---|---|
| | Trial 1 | Trial 2 | Average |
| 0.5 | 18 | 12 | 15 |
| 1 | 24 | 18 | 21 |
| 1.5 | 36 | 24 | 30 |
| 2 | 45 | 30 | 37.5 |
| 2.5 | 51 | 39 | 45 |
| 3 | 60 | 45 | 52.5 |
| 4 | 62 | 46 | 54 |
| 5 | 73.5 | 57.5 | 65.5 |

The analysis of the circumstances before and after flooding shows that the performance of flexible pavement continues to decline. It is concluded that because the CBR value of the subgrade was reduced by 41% as a result of the floods, the subgrade value of the pavement was unsatisfactory. Additionally, the value of the modulus of resilience continues to decline by 37% as a result of which irreversible deformation may take place. According to the results of the rutting model, ruts in the pavement grow by 20 mm for every 10% increase in the length of traffic beyond 30 msa. The findings of the fatigue model show an increase in the percentage of air voids in the road pavement, which causes pavement deformation. As a result, the fatigue value increased by 30%. According to the results above, pavement performance is diminished more severely after flooding than it was before.

By extending the research conducted by Hankare et al. (2020), Kumar et al. (2020) estimated "Design of flexible pavement's" with the aid of "IRC-37, 2012". The CBR before and after floods and traffic volume count were used for this. This was demonstrated in the traffic design vs. pavement thickness study, traffic volume and count analysis, and traffic design calculation using IRC-37, all of which were conducted in 2012. CBR of strong pavement built to a high standard is the most flood-resistant, and may be used as a pre-flood strategy. Table 2.3 displays the pavement layer's thickness both before and after flooding.

Table 2.3 Thickness of pavement layers estimated before and after flooding

(Source: Kumar et al., 2020)

| **Pavement Layer** | **Before flooding(mm) CBR=5.84** | **After flooding (mm) CBR=3.43** |
|---|---|---|
| GSB | 266.4 | 358.5 |
| GB | 250 | 250 |
| DBM | 109.62 | 133.83 |

Through laboratory tests and design simulations, Wang et al. (2014) examined the effects of flooding on pavement materials and structures and suggested improved pavement design and management techniques. They also developed a method to incorporate flood risk into the structural analysis of flexible pavements. The following factors are used to accomplish the goal: 1) A technique for including flood occurrences in pavement analysis; 2) the impact of flooding on pavement materials and structures; and 3) improved pavement design and management techniques to lessen the negative consequences of increasing flooding frequency due to global climate change. Climate data indicate a tendency toward an increase in the frequency of extreme weather events brought on by anthropogenic climate change. Heavy rains are one type of extreme weather, and when combined with increasing sea levels, they left some subtropical regions' routes vulnerable to floods. Flexible highway pavements in these areas suffer obvious damage from flooding. However, little study has been done to calculate these losses and create potential countermeasures. Flooding is proven to have a substantial impact on flexible pavement. Future climate change will seriously threaten the dependability of flexible roadway pavements by increasing the frequency of floods and increasing flooding severity. Pavement thickness and drainage systems must be properly planned, and post-flood traffic control may need to be implemented, in order to lessen the negative consequences of flooding. Two levels of surcharge, 3 kg and 5 kg, were placed on the top of the specimens to simulate the static loads of pavements (as shown in figure 2.4).

Figure 2. 1 Experiment to test the volume change of soaked soil specimens with surcharges (Source: Wang et al., 2014)

The load-induced responses of the pavement structure are calculated based on the Multilayer Elastic Theory (MET) using the Kenpave program.

Flooding-related road structural integrity loss could result in significant costs for road maintenance and reconstruction. The strength of the compacted soil, also known as the subgrade or road foundation, serves as the theoretical underpinning for the design of pavement structures. As a result, the subgrade plays a crucial role in the structural structure of the road. The materials in each layer of the road structure become saturated when roads are submerged for an extended period of time or repeatedly, and the original state of the subgrade soils will be compromised. Ghani et al. (2016) looked at the impact of repeated submergence of the road structural systems and the length of time the road is submerged on sub-grade strength and characteristics. In this study, cohesive and cohesionless materials, two types of soil typically employed as the embankment material in road construction, were used. Various forms of inundation and loading circumstances, including recurrent inundation, were used in the California Bearing Ratio (CBR) test and the consolidation settlement test. The results showed that prolonged flooding causes subgrade soil's strength to progressively deteriorate. Similar to the previous example, a consolidation test demonstrates that when soil is submerged for an extended period of time, a quick and higher settlement may happen. These results are helpful for ideas for road design and upkeep on flood-affected road linkages.

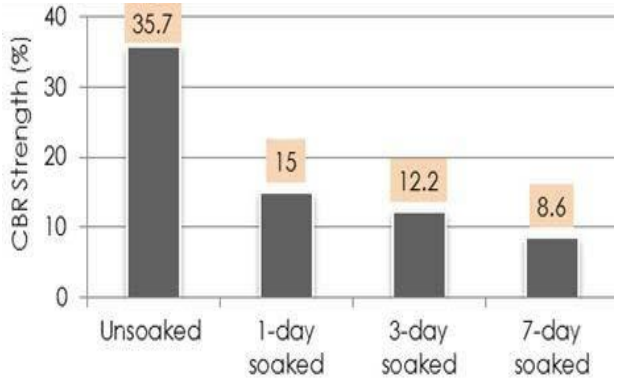


Figure 2. 2 Comparison of CBR values of inundated samples for first soil sample (Source: Ghani et al., 2016)

The comparison of soil strength for damp and unsoaked conditions is shown by the CBR strength result in figure 2.2. For soaking conditions, soil samples were submerged for 1, 3, and 7 days. Due to the saturated time for soaked soil samples, the bar chart indicates that the CBR value for the unsoaked condition is relatively higher than the CBR value for the soaked condition. For the repeated immersed condition, the bar chart in figure 2.3 shows distinct results for the soaked and unsoaked conditions. On days 1, 3, and 7, the soil samples were buried for just an hour. It demonstrates that the CBR value for the unsaturated condition was 35.7%, and the CBR values after repeatedly submerging for an hour on Day 1, Day 3, and Day 7 were 25%, 15.9%, and 18.5 percent, respectively. In essence, the results indicate that, when compared to soil samples repeatedly submerged in water, the unsoaked state still has a higher CBR strength value. In the repeatedly immersed scenario, the CBR strength was decreased on day 1 after being submerged for an hour, and the CBR value was similarly diminished on day 3 in comparison to the unsoaked sample. However, after being submerged for one hour on day 3 and day 7, the soil sample began to regain its vigour. On day 7, the CBR strength increased by 16% after submerging for an hour.

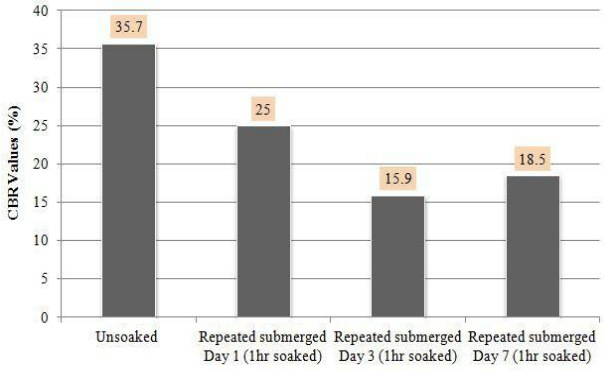


Figure 2. 3 Comparison of CBR values for repeated submergence for first soil sample (Source: Ghani et al., 2016)

## 2.2 IMPROVEMENT OF SUBGRADE AND GRANULAR LAYERS

Geotextiles are used to stabilise soft subgrade soil, according to research by Sudham et al. (2019). The goal of this study is to determine whether adding geotextile reinforcement to the subgrade soil results in an increase in strength mobilisation as measured by CBR values. The study makes use of silty expanding clay soil that was dug up during excavation at a location close to the Outer Ring Road (ORR) of Hyderabad City in Telangana State, India. Tencate Geosynthetics provided the geotextiles since HP-370 & PEC (both woven) and TS-50 (non-woven) are well-liked geosynthetic materials. These three different types of wet geotextiles are used for CBR tests (HP-370, PEC, TS-50) as shown in figure 2.4.

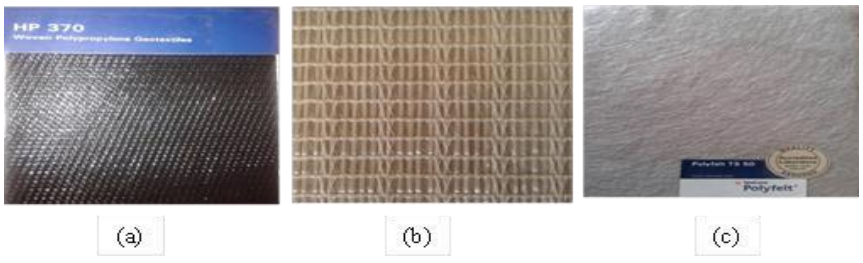


Figure 2. 4 (a).Woven Polypropylene Geotextile (HP-370) (b).Woven geotextile Poly Felt (PEC), (c).Nonwoven Geotextile (TS-50) (Source: Sudham et al., 2019)

The effectiveness of different researchers' and scientists' geotextile reinforcement materials positioned at various depths has been examined. They have only served to highlight how crucial it is to insert the geotextiles into the mould at specific depths (1/4, 1/2, 3/4, 1/3, and 2/3) in order to maximise CBR. However, in the event of clayey soils, there may be a chance to obtain the best CBR when geotextiles are positioned at various other depths of the mould. The authors of the current study have attempted to determine whether inserting the geotextiles at other feasible depths (0.2, 0.4, 0.6, and 0.8) of the mould, as stated in the section below, might result in the best CBR in two separate scenarios (ie., as single layer and as multilayer reinforcement). In Case-I of single layer reinforcement, TS-50 placed at 0.33H could provide the best CBR value of 1.61 with an 83 percent improvement in comparison to pre-reinforcement soil in the study, out of all geotextiles placed at unequal distances independently. The PEC geotextile, which could provide a CBR value of 1.42 at 0.5H after the TS-50 with a CBR value of 1.58, is the next superior geotextile. When compared to other geotextiles, TS-50 could once again provide the greatest CBR values in scenario II of multi-layer reinforcement. In particular, in all of the experimental analysis of the current study, TS-50 with 3 layers positioned at H/4 depth of the mould was the best. The CBR value is 3.92, a 345 percent increase from the research area's pre-reinforced soil. The PEC geotextiles, which could only provide 2.8 at the same depth, are the second best geotextiles. Two layers of reinforcement performed worse at H/3 depth of the testing mould than three layers of reinforcement did. Overall, both for single layer reinforcement and multi-layer reinforcement, the TS-50 (Non-woven) can be regarded as the best geotextile. When TS-50 is positioned closer to the mold's surface as opposed to farther inside the mould, the highest CBR values may be obtained.

The process of enhancing the subgrade soil's load bearing capability and engineering qualities to sustain structures and pavements is known as soil stabilisation. In this study, Ogundare et al. (2018) investigated the use of geotextile as reinforcement to stabilise two soil samples (lateritic and clay). Particle size analysis, the Atterberg Limit test, the specific gravity test, the compaction test, and the California Bearing Ratio test were all conducted as part of geotechnical testing. The American Association of State and Highway Transportation Officials (AASHTO) classifies the two soil samples as A-7-6 and A-7-5, which are deemed to be "poor" subgrade materials. To assess the strength of the soil samples, CBR tests were carried out both with and without non-woven geotextiles, with the non-woven geotextiles being positioned in a single layer at a depth of H/4 from the top and base surfaces of the soil.

The results showed that adding non-woven geotextile to the soil made the soil samples stronger since those placed at depth H/4 from the top surface had higher CBR values (15.1 percent and 19.6 percent) than those placed at depth H/4 from the base surface (14.1 percent and 18.2 percent). The trial outcomes clearly show that the presence of geotextiles raises the soil's CBR value; as a result, geotextiles should be used as a modernised method of enhancing road construction on subpar soils and to thin out pavement layers.

For engineering purposes including paving roads and highways, building dams, and filling material, certain laterite soil is a subpar material. To make laterite soil stronger for use in the field, stabilisation is necessary. Zeolite and waterglass may be used as stabilising agents due to their pozzolanic qualities. Analyzing the strength and bearing capacity of laterite soil stabilised by waterglass-activated zeolite and reinforced with geogrid is the goal of Harianto's study from 2022. Zeolite concentrations of 4, 8, 12, 16, and 20 percent, waterglass concentrations of up to 2, 4, and 6 percent, and curing periods of 0–7–14–28 days were used to generate the soil sample. Additionally, the container with the ideal composition determined by the compressive strength (UCS) and California bearing test (CBR) tests was used for the physical model test. The subgrade layer with the subpar CBR value was placed on top of the stabilised subbase layer with geogrid reinforcement. The findings demonstrated a significantly improved compressive strength (UCS) of stabilised soil after a 7-day curing period. In comparison to untreated soil, the CBR value also rose with additive content and curing time. According to the physical model test results, stabilised laterite soil with additives and geogrid reinforcement (ZW-geogrid) as a subbase layer performs more optimally in supporting the load than sand-gravel mixtures.

Due to its cohesive structure at relatively low moisture content, clay is a fine-grained soil that is plastic. Clay soils have a low CBR value and alternately expand and shrink as a function of moisture content. The introduction of geosynthetics as layers stabilised the subgrade in the study by Jayakumar et al. (2020). The geosynthetic materials employed are non-woven geotextiles and geogrids layers. Engineering characteristics of the clay specimen are assessed, including shear strength, CBR value, and index characteristics like Atterberg limits and grain size distribution. When the geogrid was positioned at the top and middle, the CBR Test result increased by 4 and 5.56 percent, respectively, from the 3.54 percent recorded for the control sample. When geotextile and geogrid are used as a combined layer, geogrid's performance is

improved. The results of the CBR test performed across the combined strata located at the top and middle are 6.31 and 6.9 percent, respectively.

Road lengths in India have significantly increased, necessitating the use of quick, affordable, and environmentally friendly construction techniques. As a result, the usage of additives during various phases of pavement building has become increasingly important over time. The primary characteristics and uses of geotextiles are soil mass reinforcement, drainage, separation, subgrade stability, etc. The two primary types of geotextiles are woven and nonwoven. In their 2016 investigation, Raut et al. used woven geotextile produced locally. During testing, geotextile was positioned at various depths of the samples. The CBR readings showed improvements. As a result, the pavement thickness with Geotextile at different depths was much less than without Geotextile. When Geotextile was inserted in the centre of the CBR mould rather than at different depths, the results were significantly better. Results from the CBR values so given using Geo textiles at different soil sample depths are variable.

1) For samples where geotextile is not used and pavement thickness is higher, the CBR value is comparably lowest.
2) The CBR value obtained for the sample using geotextile is higher than the sample using geotextile without it, resulting in a reduction in pavement thickness.
3) The sample with the highest CBR value has Geotextile placed at a depth of 6 cm (middle) in the CBR mould, resulting in the thinnest pavement possible.
4) By using geotextile, the pavement thickness is decreased.
5) Geotextile use thus enhances and stabilises the sub base characteristics.

The impact of adding non-woven polyester geotextile on the strength behaviour of weak subgrade soil is presented by Shukla et al. in 2021. In order to determine the ideal combination and location of reinforcement based on the results of the California bearing ratio, the geotextile sheets are positioned in single and multiple layers at various depths of soil subgrade. In comparison to lower layers of subgrade, soil samples reinforced with geotextile show greater improvements in CBR, with a maximum increase of 70% corresponding to double layer geotextile at 0.2 and 0.4 H depth from the top of the mould.

## 2.3ANALYSIS

Pavement premature failure is a severe issue that affects many nations, although the causes can vary. The majority of design procedures assume that the subgrade is lying approximately 500 mm above the high flood level. But heavy rainfall causes a segment of the pavement, or even the entire structure, to be submerged in several areas of the country. Low volume highways are particularly problematic because pavements are typically built on the available land without embankment. The Resilient Modulus (MR) of the pavement layers is a significant factor, and the Indian Roads Congress (IRC) provides pavement design sections for various circumstances. In the study by Priyanka et al. (2015), significant cases of MR values being reduced as a result of pavement submersion are taken into consideration. The IRC SP 72 for low volume roads suggests various subgrade and traffic conditions, which are analysed in the KENPAVE software package under the assumptions of a 25%, 50%, and 75% drop in $M_R$ values. According to the findings, all serious cases show a significant increase in stress and strain values and a sharp decrease in fatigue and rutting life. A result larger than one for the damage ratio—which is calculated as the ratio of actual load repetitions to permitted load repetitions—indicates pavement failure. The research reveals that when the $M_R$ values are reduced, the pavement constructions for ordinary instances collapse, hence design has to be modified in these situations.

Visvanathan et al(2020) .'s exploratory study focuses on how full-scale coir-reinforced low volume roads respond to static loading. The 1.736 km test track is made up of a control section, eight reinforced sections, two different kinds of coir geotextiles, and subbase with varied densities. For evaluation, a review of the general performance of coir geotextile-reinforced sections is performed under static plate load tests, California Bearing Ratio testing, geogauge tests, and dynamic cone penetration tests. The study compares the results of tests that were run on an unreinforced test track to those that were run on a reinforced test track. The findings show that the bigger apparent opening size geotextile performs less well than the finer mesh geotextile. A woven coir geotextile with a mass per unit area of 740 g/m2 can increase the elastic modulus of the subgrade by up to 112%, whereas a geotextile with a mass per unit area of 365 g/m2 can increase it by up to 70%. The elastic modulus values are calculated from the various field tests, and KENPAVE software is used to do an overall damage analysis. The analysis shows that employing coir geotextile as reinforcement results

in a noticeable reduction in the aggregate layer thickness. Therefore, using coir geotextiles as reinforcement in pavements can aid in lowering the demand for and consumption of quickly decreasing natural resources.

Engineers and designers frequently employ soil stabilisation to improve the qualities of soil with various stabilisers. Utilizing natural fibre in the soil as reinforcement has been a successful method since ancient times. The impact of adding Arecanut coir to the soil mixture in randomly spaced chunks is seen in the study by Lekha et al. (2014). By stabilising soil using arecanut coir and a binding substance, its engineering qualities and bearing capacity are improved (cement). A few studies on fibre reinforcing were mentioned together with the information that was gathered on trials and research on the behaviour of soil cement mixtures. The current study mainly focuses on the durability test and physical evaluation of soil cement mixtures reinforced with Arecanut coir. Coir content was varied from 0.2% to 1% with an increment of 0.2%. For further improvement, a uniform dosage of 3% cement was added to soil. Laboratory tests including the Unconfined Compressive Strength (UCS), California Bearing Ratio (CBR), durability and fatigue behaviour, were conducted as per standards. The test results indicated that the improvement in characteristics of the soil cement coir mixtures were functions of coir dosage, soil type and curing days. One percent Arecanut coir and three percent cement passed the durability test. Using KENPAVE software, the stress strain values and damage assessments were calculated for the greater dosage of Arecanut coir. The Arecanut coir reinforced cement soil mix can be used for low volume roads, according to the results, and a few design scenarios have been presented.

The nation's social, economic, and industrial development depends heavily on the road transportation system. Different vehicle classes use roads, which causes the pavement to deteriorate owing to early deterioration. Fatigue cracking and rutting deformation cause bitumen pavement to deteriorate. This cleared the path for the creation of software like IITPAVE, which calculates the stress and strain values at crucial points on various pavement layers. The study by Kumar et al. (2020) intends to gather field data on subgrade soil CBR values and traffic studies in order to develop flexible pavement in accordance with IRC: 37-2012. It is then examined afterwards using the IITPAVE Software to see if it complies with the particular requirements. The World Bank has conducted a global study to broaden the use of the HDM-3 Model and to offer an organised system approach to road management with flexible and user-friendly software tools. As a result, a brand-new set of highway building

and management tools known as HDM-4 Software has been created, combining numerous new capabilities to function globally with any engineering and environmental conditions. In this project, the use of HDM-4 for project analysis of the 56.53 kilometre National Highway NH-234 is briefly described. To forecast road deterioration, the HDM-4 tool gathers information on current road conditions, traffic volume, axle surveys, etc. Based on the Economic Internal Rate of Return (EIRR) and Economic Net Present Value (ENPV) values, HDM-4 simulates the utilisation of the best choices.

Using the KENLAYER software tool, Rind et al. (2019) examined the effects of rutting and fatigue distresses on a flexible pavement. The NHA (N-55) portion of road in Sehwan, Pakistan, was used as a reference pavement to achieve that goal. By varying bituminous course thicknesses by around 25%, the pavement was examined. KENLAYER software was used to examine 20 cross-sections for premature failures due to rutting and fatigue. The micro stresses decreased and the capability for more loading repetitions rose as the asphaltic wearing course and asphaltic base course thicknesses increased. Micro stresses increased and the allowed for the number of loading repetitions dropped as the thickness of the asphaltic wearing course and base course decreased.

## 2.4 RESEARCH GAP IDENTIFICATION

- Estimation of the performance parameters (rutting and fatigue lives) for different combinations of layer thicknesses of flexible pavement using pavement design softwares and comparison of the same is limited to only a few studies.
- The application of non-woven polyester geotextile as subgrade material is limited to only a few literatures and the effect of depth of placement of the same in strength and performance needs to be focused more**.**

# CHAPTER 3

# METHODOLOGY

## 3.1 GENERAL

Designers are switching from the outdated empirical design method to the new mechanistic empirical (M-E) pavement design procedure in order to create pavement structures effectively and efficiently. The pavement reactions in terms of stresses and strains in M-E design have a higher impact on performance forecasting. Over the past fifty years, experts have created a large number of theoretical equations to forecast how the pavement will react to various loading scenarios. To calculate the necessary pavement thickness for a set of design parameters, M-E design combines the aspects of mechanistic modelling with performance data. The main inputs into the mechanistic model are the traffic loading and material characteristics of various pavement layers. The pavement damage (rutting and fatigue cracking) is calculated using transfer functions or performance equations after the model predicts the mechanical reactions of the pavement in terms of stress and strain. If the level of pavement damage exceeds the previously established permitted limit, the process is repeated with increased pavement thickness. In Figure 3.1, the technique used for this investigation is depicted. According to IRC guidelines (IRC: 37-2018), the flexible pavement is developed using an empirical method that primarily relies on the CBR value of the subgrade soil and design tables to calculate the overall pavement thickness. Flexible pavement is designed in accordance with IRC: 37-2018 rules, and IITPAVE and KENPAVE are used to analyse the design. Modeled as an elastic multilayer structure is the flexible pavement. The pavement is analysed using the mechanistic empirical software packages IITPAVE and KENPAVE. The pavement inputs needed for the computation of stresses, strains, and deflections caused by a load applied at the pavement's surface are elastic modulus, Poisson's ratio, and thickness of each layer. Crucial strain positions are depicted in Figure 3.2, and stresses and strains at critical points are computed using the linear layered elastic model. According to these recommendations, the crucial mechanistic parameter for preventing subgrade rutting is the vertical compressive strain on top of the subgrade. The causative mechanistic parameter that must be limited to control bottom-up cracking in bituminous layers is assumed to be the horizontal tensile strain at the bottom of the bottom bituminous layer.

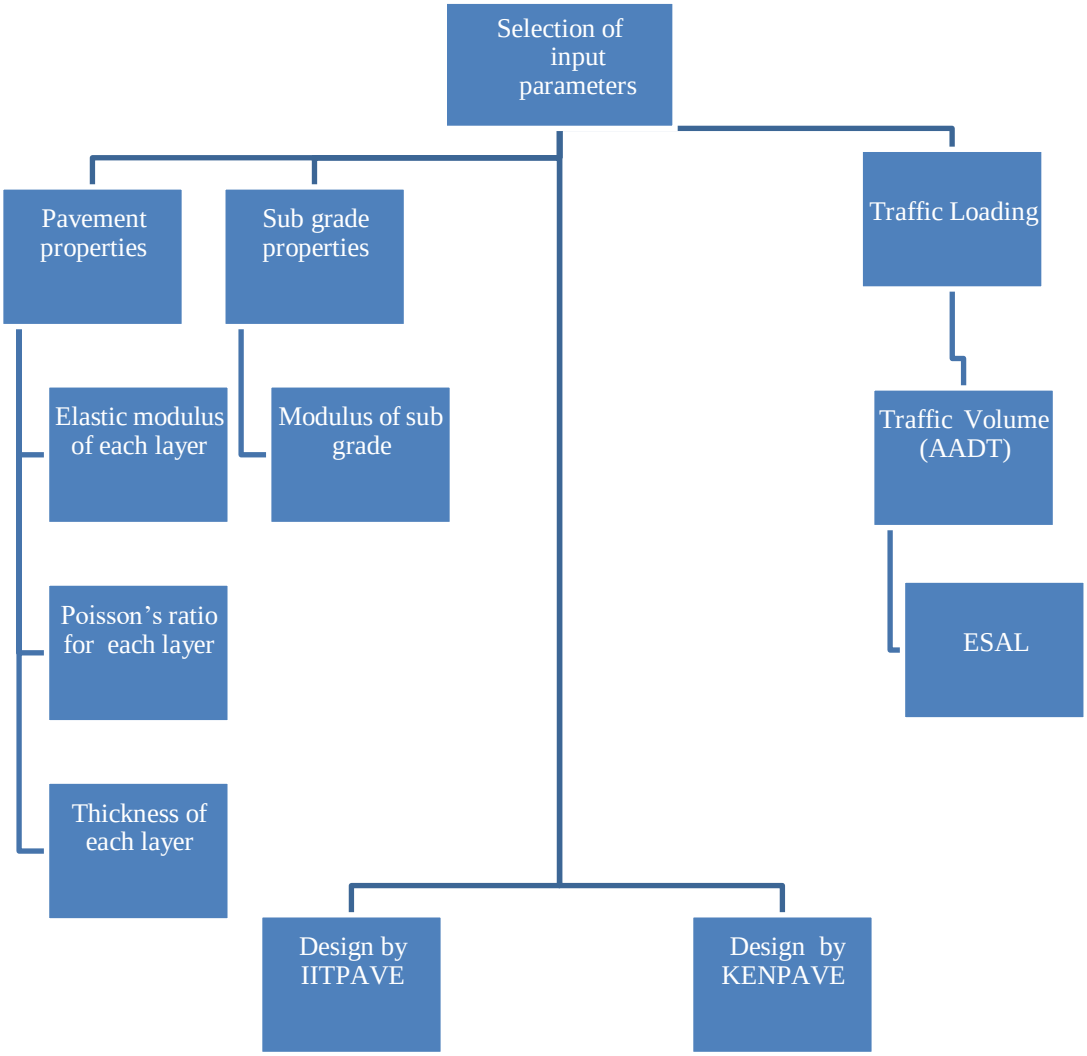


Figure 3. 1 Flowchart of design methodology adopted in IITPAVE and KENPAVE

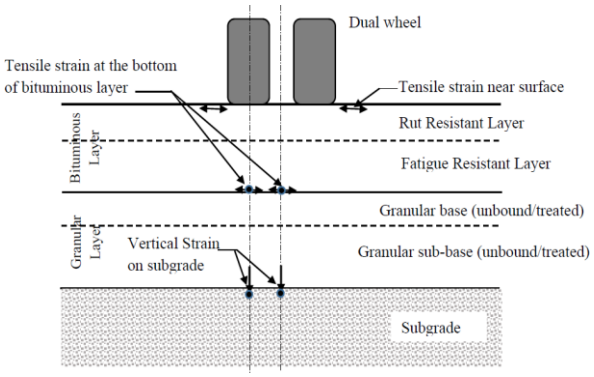


Figure 3. 2 A pavement section with bituminous layer(s), granular base and GSB showingthe locations of critical strains (Source: IRC: 37-2018)

## 3.2 RESILIENT MODULUS OF THE SUBGRADE

Resilient modulus, which is measured taking into account only the elastic (or resilient) component of the deformation (or strain) of the specimen in a repeated load test is considered to be the appropriate input for linear elastic theory for the analysis of flexible pavements. The resilient modulus of soils can be determined in the laboratory by conducting the repeated tri-axial test as per the procedure detailed in AASHTO T307-99. Since this equipment are usually expensive, the following relationships given in equation 3.1 and 3.2 may be used to estimate the resilient modulus of subgrade soil (MRS) from its CBR value.

$M_{RS} = 10.0 * CBR$ for $CBR \leq 5$ % (3.1)

$M_{RS} = 17.6 * (CBR)^{0.64}$ for $CBR > 5$ % (3.2)

Where,

$M_{RS}$ = Resilient modulus of subgrade soil (in MPa).

CBR = California bearing ratio of subgrade soil (%)

Poisson's ratio value or subgrade soil may be taken as 0.35.

## 3.3 RESILIENT MODULUS OF GRANULAR LAYER

The elastic/resilient modulus value of the granular layer is dependent on the resilient modulus value of the foundation or supporting layer on which it rests and the thickness of the granular layer. A weaker support does not permit higher modulus of the upper granular layer because of the larger deflections caused by loads result in de- compaction in the lower part of the granular layer. Equation 3.3 may be used for the estimation of the modulus of the granular from its thickness and the modulus value of the supporting layer.

$M_{RGRAN} = 0.2(h)^{0.45} * M_{RSUPPORT}$ (3.3)

Where,

h = thickness of granular layer in mm

$M_{RGRAN}$ = resilient modulus of the granular layer (MPa)

$M_{RSUPPORT}$ = (effective) resilient modulus of the supporting layer (MPa)

The granular base and granular sub-base are considered as a single layer for the purpose of analysis and a single modulus value is assigned to the combined layer.

## 3.4 PERFORMANCE CRITERIA

The following performance criteria are used in the study for the design of bituminous pavements obtained from IRC: 37-2018.

### 3.4.1 Subgrade rutting criteria

An average rut depth of 20 mm or more, measured along the wheel paths, is considered as critical or failure rutting condition. The equivalent number of standard axle load (80 kN) repetitions that can be served by the pavement, before the critical average rut depth of 20 mm or more occurs, is given by equations 3.4 and 3.5 respectively for 80 % and 90 % reliability levels.

$N_R = 4.1656 \times 10^{-08} [1/\varepsilon_v]^{4.5337}$ (for 80 % reliability) (3.4)

$N_R = 1.4100 \times 10^{-08} [1/\varepsilon_v]^{4.5337}$ (for 90 % reliability) (3.5)

Where,

$N_R$ = subgrade rutting life (cumulative equivalent number of 80 kN standard axle loads that can be served by the pavement before the critical rut depth of 20 mm or more occurs)

$\varepsilon_v$ = vertical compressive strain at the top of the subgrade calculated using linear elastic layered theory by applying standard axle load at the surface of the selected pavement system.

### 3.4.2 Fatigue cracking criteria for bituminous layer

The performance equations proposed in IRC: 37 - 2018 are similar to the equations proposed in the asphalt institute method of flexible pavement design. These equations were incorporated into IRC: 37 guidelines from the revision made in the

year 2001. A new set of coefficients were proposed for designing with 90% reliability.

$$N_f = 0.711 * 10^{-4} * [1/\varepsilon_t]^{3.89} * [1/M_{Rm}]^{0.854} \quad (3.6)$$

Where,

$M_{Rm}$ = Resilient modulus of bituminous layer (Mpa)

$\varepsilon_t$ = Horizontal tensile strain at the bottom of bituminous layer (estimated using IITPAVE software)

## 3.5 VARIATION OF THICKNESS OF PAVEMENT LAYERS

In this section the effect of variation in Asphaltic concrete layer course and Granular base and subbase course thicknesses by ±25% on the pavement performance was examined. The effect of CBR variation of subgrade on the pavement life was also examined. The single axle with dual wheel load condition and performance models of 90% reliability were considered. The single wheel load of 20000 N and contact pressure of 0.56MPa were given as the load inputs in IITPAVE where as in KENLAYER contact radius of 10.66 cm and contact pressure of 560 kPa were taken as load inputs. The elastic modulus of asphalt concrete layer course, granular layer course, and subgrade were 3000 MPa, 96.63 MPa, and 37.1 MPa respectively (for a conventional CBR of 3.71). The poisson's ratio is taken as 0.35 for all pavement layers. By altering and combining these thicknesses we observed that there is total twenty (20) probable cross-sections and one original section of a pavement that will be analysed using KENLAYER and IITPAVE software. Details of each cross-section are provided in Table 3.1.

The strains observed from KENLAYER and IITPAVE software helped in calculating number of load repetitions to prevent rutting and fatigue failure by using IRC equations. Section of pavement that gave maximum value of Nr and Nf was considered as best section of pavement with respect to pavement responses.

The snapshot of L Graph of designed section in KENLAYER is shown in Figure 3.3. The sample of IITPAVE input as well as KENLAYER input as a screenshot are given below in the Figure 3.4 and Figure 3.5 respectively. Similarly, the sample of

IITPAVE and KENLAYER output screenshots are shown in Figure 3.6 and 3.7 respectively.

Table 3. 1 Thickness of each designed cross-section

| **BITUMINOUS LAYER THICKNESS (mm)** | **GRANULAR LAYER THICKNESS (mm)** | **SECTION** |
|---|---|---|
| 120 | 300 | x |
| 60 | 450 | x1 |
| 60 | 375 | x2 |
| 60 | 300 | x3 |
| 60 | 225 | x4 |
| 60 | 150 | x5 |
| 90 | 450 | x6 |
| 90 | 375 | x7 |
| 90 | 300 | x8 |
| 90 | 225 | x9 |
| 90 | 150 | x10 |
| 150 | 450 | x11 |
| 150 | 375 | x12 |
| 150 | 300 | x13 |
| 150 | 225 | x14 |
| 150 | 150 | x15 |
| 180 | 450 | x16 |
| 180 | 375 | x17 |
| 180 | 300 | x18 |
| 180 | 225 | x19 |
| 180 | 150 | x20 |

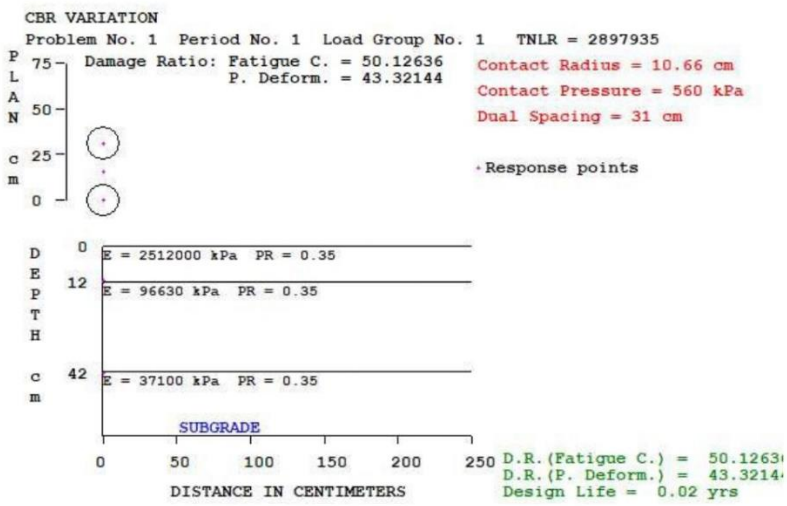


Figure 3. 3 Snapshot of L Graph of the conventional pavement section in KENLAYER

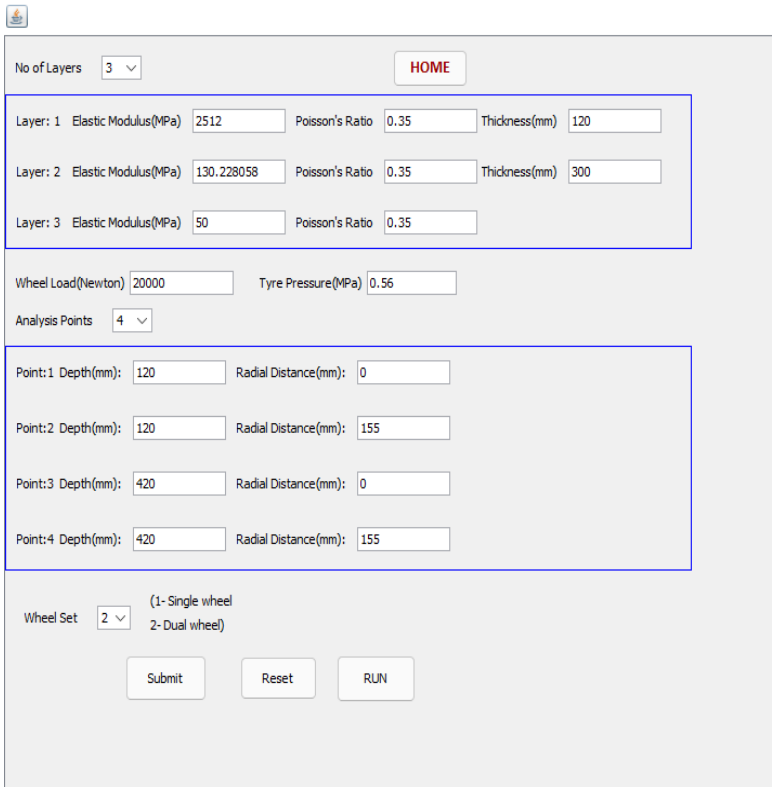


Figure 3. 4 Screenshot page of IITPAVE input page

```
NUMBER OF PROBLEMS TO BE SOLVED =  1

TITLE -Thickness variation

MATL = 1 FOR LINEAR ELASTIC LAYERED SYSTEM
NDAMA = 0, SO DAMAGE ANALYSIS WILL NOT BE PERFORMED
NUMBER OF PERIODS PER YEAR (NPY) =  1
NUMBER OF LOAD GROUPS (NLG) =  1
TOLERANCE FOR INTEGRATION (DEL) -- =  0.001
NUMBER OF LAYERS (NL)------------- =  3
NUMBER OF Z COORDINATES (NZ)------ =  2
LIMIT OF INTEGRATION CYCLES (ICL)- =  80
COMPUTING CODE (NSTD)------------- =  9
SYSTEM OF UNITS (NUNIT)-----------=  0

Length and displacement in in., stress and modulus in psi
unit weight in pcf, and temperature in F

THICKNESSES OF LAYERS (TH) ARE : 12  30
POISSON'S RATIOS OF LAYERS (PR) ARE : 0.35  0.35  0.35
VERTICAL COORDINATES OF POINTS (ZC) ARE:  12  42.0001
ALL INTERFACES ARE FULLY BONDED

FOR PERIOD NO. 1 LAYER NO. AND MODULUS ARE :    1  2.512E+06   2  1.302E+05
   3  5.000E+04

LOAD GROUP NO. 1  HAS 2  CONTACT AREAS
CONTACT RADIUS (CR)--------------- =  10.66
CONTACT PRESSURE (CP)------------- =  560
NO. OF POINTS AT WHICH RESULTS ARE DESIRED (NPT)-- =  3
WHEEL SPACING ALONG X-AXIS (XW)--------------------- =  0
WHEEL SPACING ALONG Y-AXIS (YW)--------------------- =  31

RESPONSE PT. NO. AND (XPT, YPT) ARE:  1   0.000   0.000  2   0.000  15.500
  3   0.000  31.000
```

Figure 3. 5 Screenshot page of KENLAYER input page

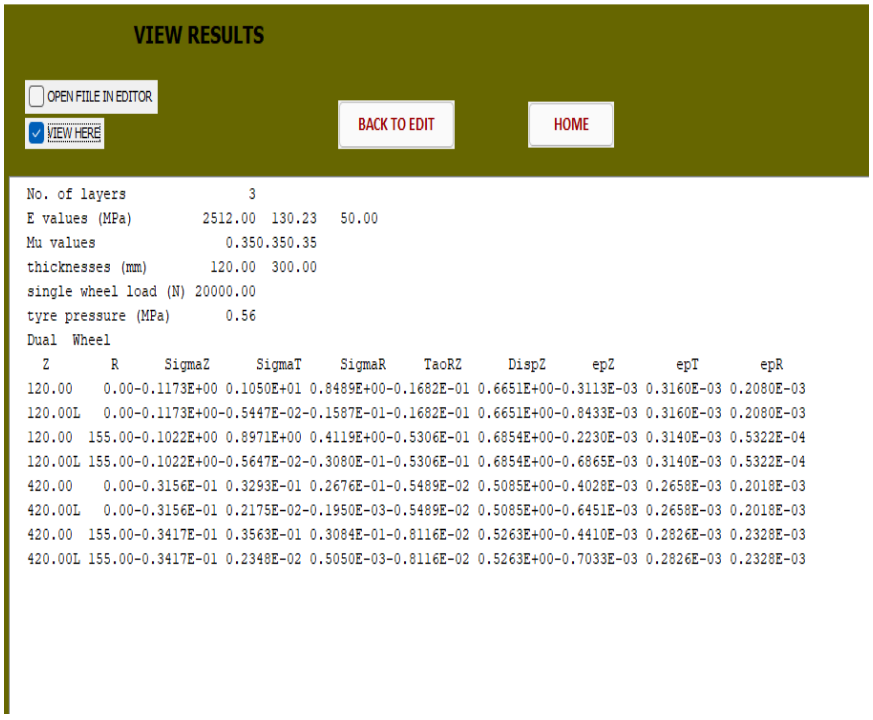


```
No. of layers                3
E values (MPa)         2512.00  130.23   50.00
Mu values                0.350.350.35
thicknesses (mm)        120.00  300.00
single wheel load (N) 20000.00
tyre pressure (MPa)       0.56
Dual  Wheel
  Z        R      SigmaZ      SigmaT     SigmaR     TaoRZ      DispZ      epZ        epT        epR
120.00    0.00-0.1173E+00 0.1050E+01 0.8489E+00-0.1682E-01 0.6651E+00-0.3113E-03 0.3160E-03 0.2080E-03
120.00L   0.00-0.1173E+00-0.5447E-02-0.1587E-01-0.1682E-01 0.6651E+00-0.8433E-03 0.3160E-03 0.2080E-03
120.00  155.00-0.1022E+00 0.8971E+00 0.4119E+00-0.5306E-01 0.6854E+00-0.2230E-03 0.3140E-03 0.5322E-04
120.00L 155.00-0.1022E+00-0.5647E-02-0.3080E-01-0.5306E-01 0.6854E+00-0.6865E-03 0.3140E-03 0.5322E-04
420.00    0.00-0.3156E-01 0.3293E-01 0.2676E-01-0.5489E-02 0.5085E+00-0.4028E-03 0.2658E-03 0.2018E-03
420.00L   0.00-0.3156E-01 0.2175E-02-0.1950E-03-0.5489E-02 0.5085E+00-0.6451E-03 0.2658E-03 0.2018E-03
420.00  155.00-0.3417E-01 0.3563E-01 0.3084E-01-0.8116E-02 0.5263E+00-0.4410E-03 0.2826E-03 0.2328E-03
420.00L 155.00-0.3417E-01 0.2348E-02 0.5050E-03-0.8116E-02 0.5263E+00-0.7033E-03 0.2826E-03 0.2328E-03
```

Figure 3. 6 Screenshot page of IITPAVE output page

RESPONSE PT. NO. AND (XPT, YPT) ARE: 1 0.000 0.000 2 0.000 15.500
3 0.000 31.000

PERIOD NO. 1 LOAD GROUP NO. 1

| POINT NO. | VERTICAL COORDINATE | VERTICAL DISP. | VERTICAL STRESS (STRAIN) | MAJOR PRINCIPAL STRESS (STRAIN) | MINOR PRINCIAL STRESS (STRAIN) | INTERMEDIATE P. STRESS (HORIZONTAL P. STRAIN) |
|---|---|---|---|---|---|---|
| 1 | 12.00000 | 0.06656 | 117.371 | 117.664 | -1050.770 | -849.256 |
| | (STRAIN) | | 3.114E-04 | 3.116E-04 | -3.164E-04 | -3.164E-04 |
| 1 | 42.00010 | 0.05089 | 31.599 | 32.530 | -2.189 | -0.731 |
| | (STRAIN) | | 6.459E-04 | 6.710E-04 | -2.664E-04 | -2.664E-04 |
| 2 | 12.00000 | 0.06860 | 102.258 | 102.258 | -897.878 | -412.433 |
| | (STRAIN) | | 2.233E-04 | 2.233E-04 | -3.142E-04 | -3.142E-04 |
| 2 | 42.00010 | 0.05267 | 34.200 | 34.200 | -2.349 | -0.504 |
| | (STRAIN) | | 7.040E-04 | 7.040E-04 | -2.829E-04 | -2.829E-04 |
| 3 | 12.00000 | 0.06656 | 117.371 | 117.664 | -1050.770 | -849.256 |
| | (STRAIN) | | 3.114E-04 | 3.116E-04 | -3.164E-04 | -3.164E-04 |
| 3 | 42.00010 | 0.05089 | 31.599 | 32.530 | -2.189 | -0.731 |
| | (STRAIN) | | 6.459E-04 | 6.710E-04 | -2.664E-04 | -2.664E-04 |

Figure 3. 7 Screenshot page of KENLAYER output page

## 3.6 DAMAGE ANALYSIS

The KENLAYER computer program applies only to flexible pavements with no joints or rigid layers. The backbone of KENLAYER is the solution for an elastic multilayer system under a circular loaded area. The software does linear elastic multi-layer analysis to obtain the results including stresses, strains and deflections. It can be applied to layered systems under single, dual, dual-tandem and dual-tridem wheel configurations with different layer behaviours like linear elastic, nonlinear elastic and visco-elastic. Damage ratio is the ratio of actual load repetitions to the allowed load repetitions and a value greater than one for this indicates pavement failure. Damage analysis shows the extent of damage of the pavement structure. Damage analysis can be made by dividing each year into a maximum of 12 periods, each with a different set of material properties. Each period can have different loading conditions, with single or multiple wheeled. The damage caused by fatigue cracking and permanent deformation in each period over all load groups can be summed up to evaluate the design life.

## 3.7 COST COMPARISONS (DSR(VOL-2), 2021)

The costs of material and construction of pavement layers are presented here in table 3.2 as per the rates specified in the Delhi schedule of rates (DSR, 2021) published by the CPWD.

Table 3. 2 Rates for construction of different pavement layers (Source: DSR, 2021)

| Sl. No. | Material description | Cost per cubic metre in Rs. | As per clause |
|---|---|---|---|
| 1 | Granular sub- base (GSB) | 2658.65 | 16.78, page 339 |
| 2 | Wet mix macadam (WMM) | 2803.65 | 16.79, page 339 |
| 3 | Dense Bituminous macadam (DBM) | 10013.30 | 16.54, page 334 |

The cost estimate for the selected layer combinations to withstand the design traffic are to be calculated as per 1 m length and 9 m width of the pavement section. So, a typical volume estimate for pavement layers will be length x width x thickness, where length is considered as 1 m and width as 9 m. Hence, the volume of mix required is 9*h where h is the thickness of the layer in m.

## 3.8 DESIGN FOR GEOGRID REINFORCED FLEXIBLE PAVEMENT (IRC:SP:59-2019)

A geogrid's primary stabilization mechanism is lateral restraint of the subbase or base materials through a process of interlocking the aggregate and the apertures of the geogrid. The level of lateral restraint that is achieved is a function of the type of geogrid and the quality and gradation of the base or subbase material placed on the geogrid. To maximize performance of the geogrid, a well-graded granular base or subbase material should be selected that is sized appropriately for the aperture size of the geogrid. When aggregate is placed over geogrid, it quickly becomes confined within the apertures and is restrained from punching into the soft subgrade and shoving laterally. This results in a "stiffened" aggregate platform over the geogrid. Very little deformation of the geogrid is needed to achieve the lateral restraint and reinforcement.

IRC:37 provides design procedure for unreinforced section. As many of the parameters used are still empirical, the equation requires modification to include the benefit of reinforcement in the pavement layers. Hence to take the advantage of empirical and mechanistic empirical methodologies, reinforced pavement design shall be done in the following procedure. Design for geogrid reinforced pavement design procedure shall be done in two parts:

a) Determine the conventional unreinforced pavement section as per IRC:37 for given subgrade CBR, design traffic.

b) Determine the improved layer parameters by inclusion of geogrid in different layers.

Using these improved parameters, reinforced section shall be designed with same methodology as per IRC:37 and calculation of fatigue and rutting resistance of geogrid reinforced pavement section.

The detailed design procedure for geogrid reinforced pavement section.

1. Determine the sub grade CBR and design traffic load for which the flexible pavement is to be designed. Unreinforced section thickness shall be determined according to the IRC:37 for specified sub grade CBR and Design Traffic.

2. Resilient moduli $M_{R\_GB}$ and $M_{R\_GSB}$ are evaluated for the base and sub-base.

3. The tensile horizontal and vertical strains are evaluated for the conventional section at Points A and B for the given subgrade CBR and traffic/pavement life.

4. Structural layer coefficients $a_2$, $a_3$ for granular base and subbase layer of unreinforced section shall be determined from its resilient modulus using following equations from AASHTO 1993.

$$a_2 = 0.249 (\log_{10} M_{R\_GB}) - 0.977 \quad (3.7)$$

$$a_3 = 0.227 (\log_{10} M_{R\_GSB}) - 0.839 \quad (3.8)$$

Where $M_{R\_GB}$ and $M_{R\_GSB}$ are resilient modulus of base and subbase layers

5. Benefit of inclusion of geogrid reinforcement in the pavement layers will be represented in improvement of resilient modulus of respective layer. Consider the layer within which the geogrid is placed, base, or sub-base, or both. Accordingly, the corresponding structural layer coefficient(s) is/are modified by multiplying by the corresponding linear coefficient ratios.

$$LCR_2 a_2 = 0.249 (\log_{10} M^1_{R\_GB}) - 0.977 \quad (3.9)$$

$$LCR_3 a_3 = 0.227 (\log_{10} M^1_{R\_GSB}) - 0.839 \quad (3.10)$$

Where $M^1_{R\_GB}$ and $M^1_{R\_GSB}$ are modified resilient modulus of base and subbase layers. The indicative range of LCR for CBR<3% is 1.2 to 1.8 and for CBR>3% is 1.2 to 1.6.

6. From equation (3.9) and/or (3.10), $M^1_{R\_GB}$ and/or $M^1_{R\_GSB}$ are evaluated.
7. $M^1_{R\_GB}$ and/or $M^1_{R\_GSB}$ are then used to determine the reduced thicknesses of the pavement components.
8. Further, these values are imposed in the IRC recommended IITPAVE software and evaluated for the strain values as shown in below figure 3.8.
9. By using critical tensile strain and compressive strain induced at the bottom of the bituminous course and top of the sub grade respectively, the allowable traffic should be determined for fatigue and rutting failures using equations from IRC:37.
10. If obtained strain values are less than the permissible strain values the section is safe for pavement life in rutting and fatigue and may be adopted for the construction.

The optimum geogrid location for lower thicknesses (< 150 mm) shall be at the bottom of the layer and for the higher thicknesses (> 150 mm) it shall be at 1/3rd to half of thickness from top. For very soft subgrades (CBR≤3%), optimum performance occurs with two layers of geogrids when geosynthetic shall be used in separate layers of base and sub base.

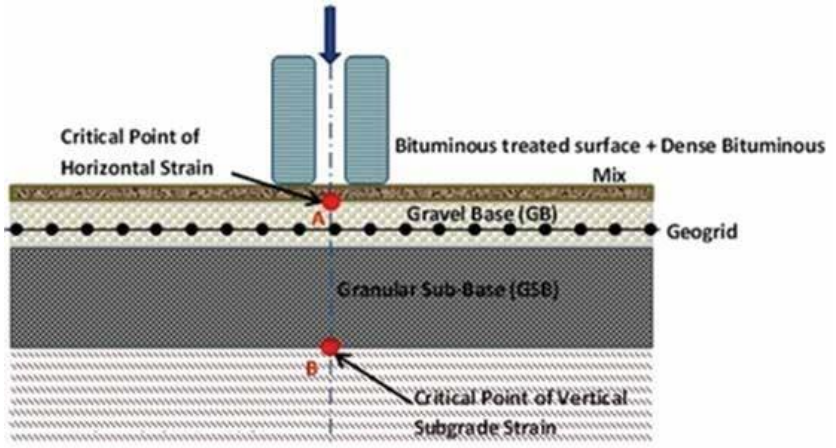


Figure 3. 8 Critical Points for Evaluation of Horizontal and Vertical strains
(Source: IRC-SP:59, 2018)

## 3.9 DESIGN OF FLEXIBLE PAVEMENT FOR EFFECTIVE CBR

Sometimes, there can be a significant difference between the CBR values of the soils used in the subgrade and in the embankment layer below the subgrade. Alternatively, the 500 mm thick subgrade may be laid in two layers, each layer material having different CBR value. In such cases, the design should be based on the effective modulus/CBR value of a single layer

subgrade which is equivalent to the combination of the subgrade layer(s) and embankment layer. The effective modulus/CBR value may be determined as per the following procedure which is a generalization of the approach presented earlier in an Indian Roads Congress publication.

(i) Using IITPAVE software, determine the maximum surface deflection (δ) due to a single wheel load of 40,000 N and a contact pressure of 0.56 MPa for a two or three layer elastic system comprising of a single (or two sub-layers) of the 500 mm thick subgrade layer over the semi-infinite embankment layer. The elastic moduli of subgrade and embankment soils/layers may be estimated from equations 3.1 and 3.2 using their laboratory CBR values. Poisson's ratio (μ) value may be taken as 0.35 for all the layers.

(ii) Using the maximum surface deflection (δ) computed in step (i) above, estimate the resilient modulus $M_{RS}$ of the equivalent single layer using equation 3.11.

$$M_{RS} = \frac{2(1-\mu^2)pa}{\delta} \qquad (3.11)$$

Where, p = contact pressure = 0.56 MPa

a = radius of circular contact area, which can be calculated using the load applied (40,000 N) and the contact pressure 'p' (0.56 MPa)

= 150.8 mm

μ = Poisson's ratio

## 3.10 SITE SELECTION

Soil samples were collected from 3 flood-prone areas in Alappuzha district. The locations are Pallathuruthy, Kainakary and Mampuzhakary (AC-road) (as shown in figures 3.9, 3.10, 3.11, 3.12, 3.13). The top soil was removed up to a depth of 10 cm and samples of approximately 2 kg weight was taken from the 3 locations. These three locations were chosen since they were the most affected, devastated areas in Alappuzha during the 2018 and 2019 Kerala floods. Heavy rain and sea erosion wreaked havoc in different parts of the district during the year 2021. Low-lying areas in the district have been inundated. Kainakary, a taluk in Kuttanad which is a below sea level area spread across Alappuzha and Kottayam districts, is literally swallowed by rain water. The situation was not much different in other parts of the district like Chengannur, Mampuzhakary, Ambalappuzha, Chungam, Cherthala etc. Pallathuruthy is a water

bound region surrounded by the Vembanad Lake. Also, the Pallathuruthy Canal passes through the region. The A-C canal, which runs along 99% of the length of the road on its southern side is meant to empty the flood waters of upper Kuttanad into the Nedumudy river and the Pallathuruthy river near Alappuzha, which reach the Vembanad lake but did not come into effect so far, resulting in the submerging of the road even when the symptoms of a flood is seen in monsoon. The AC road is prone to flooding during monsoon seasons in Kerala. As the road mostly passes through low-lying areas of Kuttanad, the road traffic is affected during heavy rains as parts of the road will be submerged in flood waters from Kuttanad.

Figure 3. 9 Location 1- Pallathuruthy, Alappuzha

Figure 3. 10Area from where soil sample is collected in Pallathuruthy, Alappuzha

Figure 3. 11 Location 2- Kainakary, Alappuzha

Figure 3. 12 Collection of soil sample from Kainakary, Alappuzha

Figure 3. 13 Location 3- Mampuzhakary (AC road)

## 3.11 INITIAL TESTS CONDUCTED

### 3.11.1 Specific gravity

Specific gravity tests were performed on the respective soil samples collected from the three locations. The Pycnometer was used for determination of specific gravity of soil particles of both fine grained and coarse grained soils. The specific gravity ($G_S$) of a soil refers to the ratio of the solid particles' unit weight to the unit weight of water. Table 3.3 shows the range of specific gravity for different soil types. Figure 3.14 shows the specific gravity test performed using pycnometer.

Table 3. 3 Specific gravity of soil particles (Source: Dr. K.R Arora, Soil mechanics and foundation engineering, 7th edition)

| Soil type | Specific gravity |
|---|---|
| Sand | 2.65-2.68 |
| Silty sands | 2.66-2.70 |
| Silt | 2.66-2.70 |
| Inorganic clays | 2.68-2.80 |
| Organic soils | May be < 2.0 (2.2 - 2.64) |


Figure 3.14 Specific gravity test performed using pycnometer

### 3.11.2 Dry Sieve analysis (particle size determination)

The grain size analysis test is performed to determine the percentage of each size of grain that is contained within a soil sample, and the results of the test can be used to produce the grain size distribution curve. This information is used to classify the soil and to predict its behavior. Sieve analysis is a method that is used to determine the grain size distribution of soils that are greater than 0.075 mm in diameter. It is usually performed for sand and gravel but cannot be used as the sole method for determining the grain size distribution of finer soil. The data may also be useful in developing relationships concerning porosity and packing. Information obtained from the particle size analysis (uniformity coefficient $C_u$, coefficient of curvature, $C_c$, and effective size, $D_{10}$, etc.) is used to classify the soil. D10 is the particle size such that 10% of the soil is finer than this size, known as effective size. D30 is the particle size such that 30% of the soil is finer than this size. D60 is the particle size such that 60% of the soil is finer than this size. The uniformity of a soil is expressed qualitatively by a term called uniformity coefficient, Cu and is expressed as:

$$\mathrm{Cu} = \frac{\mathrm{D60}}{\mathrm{D10}}$$

The general shape of the particle size distribution curve is described by another coefficient known as coefficient of curvature(Cc) or the coefficient of gradation(Cg)

$$Cc = \frac{D30^2}{D60 \times D10}$$

Figure 3.15 shows the sieve analysis being performed in sieve shaker. The I.S sieve sizes are shown in table 3.4 below.

Table 3. 4 IS sieve sizes (Source: Dr. K.R Arora, Soil mechanics and foundation engineering, 7th edition)

| Sieve no. | Opening size(mm) |
|---|---|
| 4 | 4.75 |
| 10 | 2.00 |
| 18 | 1.00 |
| 30 | 0.600 |
| 40 | 0.425 |
| 50 | 0.300 |
| 100 | 0.150 |
| 200 | 0.075 |

Figure 3. 15 Sieve analysis test performed using various IS sieves in sieve shaker

### 3.11.3. Atterberg's limits test

The Atterberg's limits tests are generally performed for fine grained soils (ie., soil particles which are finer than 0.075 mm). The Atterberg's limits tests are liquid limit test, plastic limit test and shrinkage limit test. The liquid limit is the moisture content at which the groove, formed by a standard tool into the sample of soil taken in the standard cup, closes for 10 mm on being given 25 blows in a standard manner. This is the limiting moisture content at which the cohesive soil passes from liquid state to plastic state. The liquid limit test is performed using Casagrande apparatus. Figure 3.16 shows the soil sample collected from Kainakary about to be tested in Casagrande apparatus. Figure 3.17 shows the liquid limit test performed in Casagrande apparatus for soil sample collected from Kainakary.


Figure 3. 16 Soil sample collected from Kainakary about to be tested in Casagrande apparatus.

Figure 3. 17 Liquid limit test performed in Casagrande apparatus for soil sample collected from Kainakary

The plastic limit (PL) is determined by rolling out a thread of the fine portion of a soil on a flat, non-porous surface. It is defined as the gravimetric moisture content where the thread breaks apart at a diameter of 3.2 mm (about 1/8 inch). A soil is considered non-plastic if a thread cannot be rolled out down to 3.2 mm at any moisture possible (figure 3.18).

Figure 3. 18 Soil rolled down to threads of 3 mm diameter

## 3.12 PRELIMINARY TESTS RESULTS FOR VARIOUS LOCATIONS

### **3.12.1** Specific gravity

Table 3.5 shows the recorded observations and calculations performed to obtain specific gravity of the respective soil samples.

Table 3. 5 Observations and calculations of specific gravity test

| Soil sample designation | 1 | 2 | 3 |
|---|---|---|---|
| Locations | Pallathuruthy, Alappuzha | Kainakary, Alappuzha | Mampuzhakary, Alappuzha |
| Weight of pycnometer ($W_1$) | 0.620 | 0.620 | 0.620 |
| Weight of pycnometer + soil ($W_2$) | 1.120 | 1.016 | 1.237 |
| Weight of pycnometer + soil+ water ($W_3$) | 1.799 | 1.740 | 1.844 |
| Weight of pycnometer + water ($W_4$) | 1.487 | 1.486 | 1.487 |
| Specific gravity of soil, G | **2.66** | **2.8** | **2.4** |

### 3.12.2 Dry sieve analysis (particle size determination)

(i) Location 1- Pallathuruthy, Alappuzha

Table 3.6 shows the recorded observations of dry sieve analysis test performed for location 1 soil sample

Table 3. 6 Observations of dry sieve analysis test performed for location 1 soil sample

| Sieve size (mm) | Weight of soil retained (gm) | Percentage retained | Cumulative percentage retained | Percentage finer |
|---|---|---|---|---|
| 4.75 | 35 | 3.5 | 3.5 | 96.5 |
| 2.00 | 103 | 10.3 | 13.8 | 86.2 |
| 1.00 | 164 | 16.4 | 30.2 | 69.8 |
| 0.600 | 131 | 13.1 | 43.3 | 56.7 |
| 0.425 | 200 | 20 | 63.3 | 36.7 |
| 0.300 | 87 | 8.7 | 72 | 28 |
| 0.15 | 256 | 25.6 | 97.6 | 2.4 |
| 0.075 | 13 | 1.3 | 98.9 | 1.1 |
| Pan | 11 | 1.1 | 100 | |

Figure 3.19 shows the particle size distribution curve drawn for location 1 soil sample.

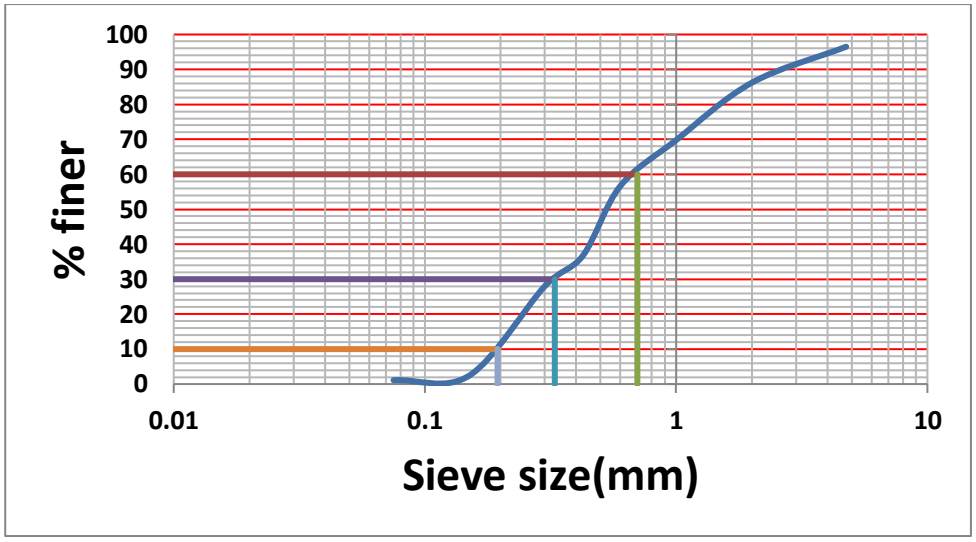


Figure 3. 19 Particle size distribution curve for location 1 soil sample

From the particle size distribution curve,

D10 = 0.19

D30 = 0.33

D60 = 0.70

Therefore, $\text{Cu} = \frac{\text{D60}}{\text{D10}}$

$= \frac{0.70}{0.19}$

$=$**3.602**

Also, $Cc = \frac{D30^2}{D60 \times D10}$

$= \frac{0.33^2}{0.70 \times 0.19}$

$=$ **0.79**

(ii) Location 2- Kainakary, Alappuzha

Table 3.7 shows the recorded observations of dry sieve analysis test performed for location 2 soil sample

Table 3. 7 Observations of dry sieve analysis test performed for location 2 soil sample

| Sieve size (mm) | Weight of soil retained (gm) | Percentage retained | Cumulative percentage retained | Percentage finer |
|---|---|---|---|---|
| 4.75 | 2 | 0.2 | 0.2 | 99.8 |
| 2.00 | 13 | 1.3 | 1.5 | 98.5 |
| 1.00 | 17 | 1.7 | 3.2 | 96.8 |
| 0.600 | 6 | 0.6 | 3.8 | 96.2 |
| 0.425 | 56 | 5.6 | 9.4 | 90.6 |
| 0.300 | 65 | 6.5 | 15.9 | 84.1 |
| 0.15 | 72 | 7.2 | 23.1 | 76.9 |
| 0.075 | 187 | 18.7 | 41.8 | 58.2 |
| Pan | 582 | 58.2 | 100 | |

Figure 3.20 shows the particle size distribution curve drawn for location 2 soil sample.

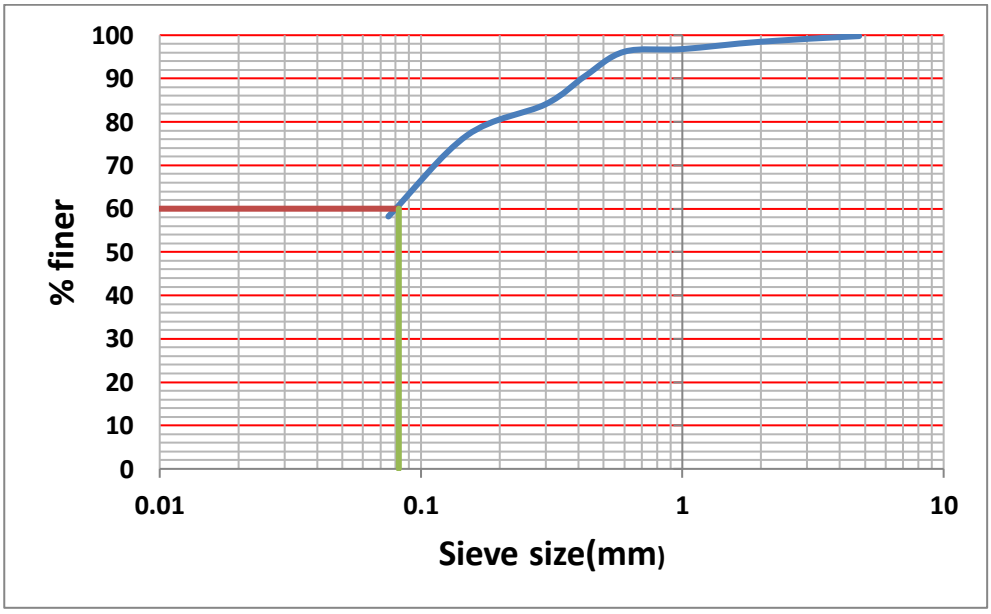


Figure 3. 20 Particle size distribution curve for location 2 soil sample

From the particle size distribution curve,

D10 = 0

D30 = 0

D60 = 0.08

Therefore, $\mathrm{Cu} = \frac{\mathrm{D60}}{\mathrm{D10}}$

= **0**

Also, $Cc = \frac{D30^2}{D60 \times D10}$

= **0**

(iii) Location 3- Mampuzhakary, Alappuzha

Table 3.8 shows the recorded observations of dry sieve analysis test performed for location 3 soil sample.

Table 3. 8 Observations of dry sieve analysis test performed for location 3 soil sample

| Sieve size (mm) | Weight of soil retained (gm) | Percentage retained | Cumulative percentage retained | Percentage finer |
|---|---|---|---|---|
| 4.75 | 51.5 | 5.15 | 5.15 | 94.85 |
| 2.00 | 51 | 5.1 | 10.25 | 89.75 |
| 1.00 | 72.5 | 7.25 | 17.25 | 82.75 |
| 0.600 | 64 | 6.4 | 23.9 | 76.1 |
| 0.425 | 69 | 6.9 | 30.8 | 69.2 |
| 0.300 | 45 | 4.5 | 35.3 | 64.7 |
| 0.15 | 385 | 38.5 | 73.8 | 26.2 |
| 0.075 | 184 | 18.4 | 92.2 | 7.8 |
| Pan | 78 | 7.8 | 100 | |

Figure 3.21 shows the particle size distribution curve drawn for location 3 soil sample.

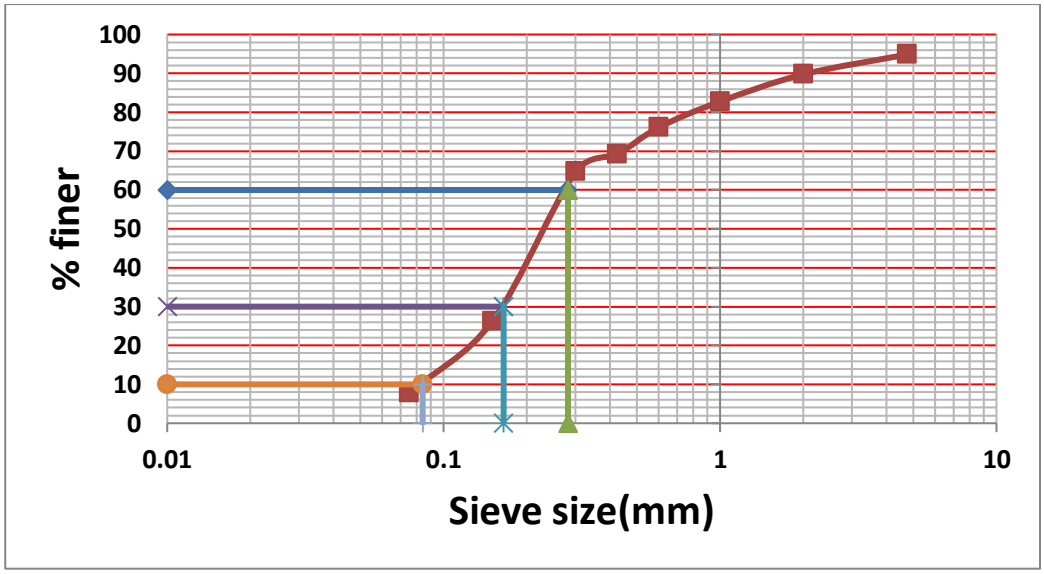


Figure 3. 21 Particle size distribution curve drawn for location 3 soil sample

From the particle size distribution curve,

D10 = 0.08

D30 = 0.16

D60 = 0.28

Therefore, $Cu = \frac{D60}{D10}$

$= \frac{0.28}{0.08}$

$=$**3.35**

Also, $Cc = \frac{D30^2}{D60 \times D10}$

$= \frac{0.16^2}{0.28 \times 0.08}$

$=$ **1.148**

**3.12.3** Atterberg limits tests

As more than 50% of the soil particles collected from location 2 (Kainakary, Alappuzha) passes through 0.075 mm sieve, the soil is observed to be fine grained. Fine grained soils are classified into silt, clay or organic soil using plasticity chart after conducting Atterberg limits test (liquid limit test and plastic limit test).

(i) Liquid limit test

Table 3.9 shows the observations recorded for liquid limit test performed using Casagrande apparatus.

Table 3. 9 Observations recorded for liquid limit test

| Trial no. | Water content (%) | Number of blows |
|---|---|---|
| 1 | 29 | 40 |
| 2 | 31 | 38 |
| 3 | 33 | 36 |
| 4 | 35 | 23 |
| 5 | 37 | 20 |
| 6 | 39 | 14 |

A graph is drawn by plotting water content in percentage on the x-axis and number of blows on the y-axis (figure 3.22). The liquid limit of the soil is the water content (in %) corresponding to 25 number of blows.

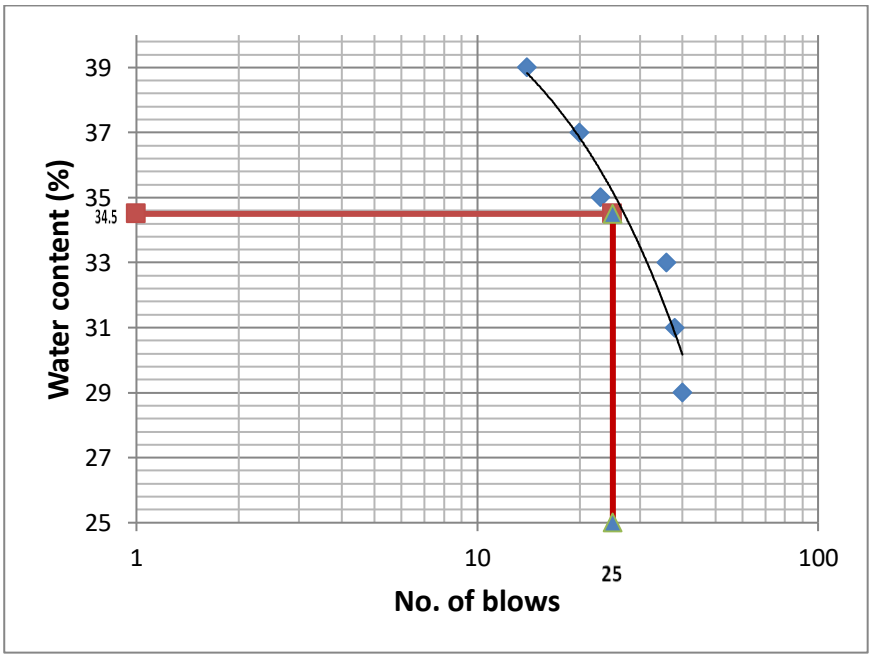


Figure 3. 22 Graph obtained for liquid limit test

Liquid limit of soil($w_L$) = **34.5%**

(ii) Plastic limit test

About 25 gram of the thoroughly mixed oven-dried soil passing through 425 micron sieve was initially taken in an evaporating dish and mixed with sufficient quantity of distilled water

Weight of container (gm) = 17.09 g

Weight of wet soil+ weight of container (gm) = 48.58 g

Weight of dry soil + weight of container (gm) = 43.41 g

Weight of water (gm) = 5.17 g

Dry weight of soil (gm) = 26.32 g

Plastic limit of soil, $w_P$ = $\frac{\text{weight of water (gm)}}{\text{dry weight of soil (gm)}} \times 100$

$= \frac{5.17}{26.32} \times 100$

$=$ **19.64%**

Plasticity Index($I_P$)

Plasticity index of soil ( $I_P$) = Liquid limit - Plastic limit

$= w_L - w_P$

$= 34.5 - 19.64$

$=$ **14.86**

## 3.13 SOIL CLASSIFICATION

### **3.13.1** General

According to the specific gravity, an analyst can have a broad idea about the type of soil. After conducting pycnometer tests, the specific gravity of soil samples collected from the 3 locations were analyzed. The soil sample obtained from location 1 (Pallathuruthy, Alappuzha) is observed to have a specific gravity of 2.66. This shows that the soil is a sandy type soil (G= 2.65 to 2.68 for sandy type soil). The soil sample obtained from location 2 (Kainakary, Alappuzha) is observed to have a specific gravity approximately equal to 2.8. This shows that the soil is an inorganic clay (G = 2.68 to 2.8 for inorganic clays). The soil sample obtained from location 3 (Mampuzhakary, AC road) is observed to have a specific gravity approximately equal to 2.4 which shows

that the soil sample is an organic soil type (G =2.2 to 2.64 or may be less than 2.0 for organic soil).

### 3.13.2 Indian Standard Classification system (ICS)

Indian Standard Classification (ISC) system adopted by Bureau of Indian Standards is in many respects similar to the Unified Soil Classification (USC) system. However, there is one basic difference in the classification of fine-grained soils. The fine grained soils in ISC system are subdivided into three categories of low, medium and high compressibility instead of two categories of low and high compressibility in USC system.

Sieve analysis was performed for the soil samples collected from the three locations and are classified based on ISC system as follows:

(i) Location 1- Pallathuruthy, Alappuzha

More than half of material (98.9%) is larger than 0.075 mm IS sieve size. Therefore, the soil is classified as coarse-grained soil. More than half of coarse fraction (96.5%) is smaller than 4.75 mm IS sieve sieve. Therefore, the soil is classified as sand. Since fines are less than 5% (1.1%), the sand would be either well-graded (SW) or poorly-graded (SP). Since, Cu calculated is 3.602 and Cc is 0.79, both values does not meet all the gradation requirements for SW (Cu > 6, 1<Cc>3 for SW). therefore, the soil is classified as **Poorly-graded sand (SP)**.

(ii) Location 2- Kainakary, Alappuzha

As more than half of the material (58.2%) is smaller than 0.075 mm IS sieve size, the soil is classified as fine-grained. Fine grained soils are classified using plasticity chart (figure 3.23). Since liquid limit of the soil is less than 35% (34.5%), the soil would have low compressibility (L).

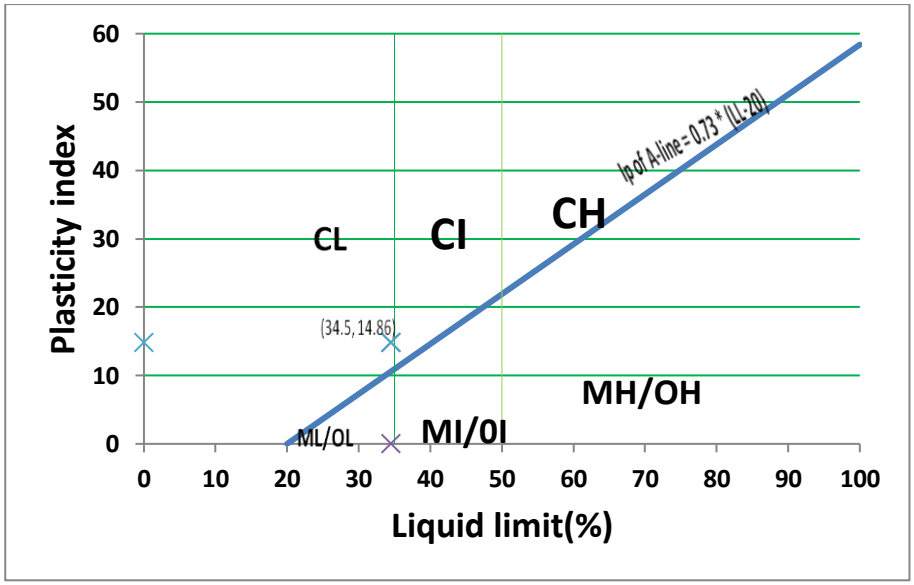


Figure 3. 23 Plasticity chart drawn for location 2 soil sample

$I_P$ of A- line = 0.73 ( $w_L$ - 20) = 0.73 (34.5 - 20)

= 10.585

$I_P$ of soil = $w_L$ - $w_P$ = 14.86

$I_P$ of A - line < $I_P$ of soil

Therefore, it is a clay soil sample

Also, liquid limit, $w_L$ = 34.5% ($w_P$< 35 for low compressibility)

Therefore, it is a **clay soil sample of low compressibility (CL)**

(iii) Location 3- Mampuzhakary (AC road)

More than half of the material (92.2%) is larger than 0.075 mm IS sieve size. Therefore, the soil is classified as coarse-grained soil. More than half of coarse fraction (94.85%) is smaller than 4.75 mm IS sieve sieve. Therefore, the soil is classified as sand. Since fine fraction are between 5% and 12% (7.8%), border line cases requiring dual symbols such as SW-SC should be applied. Cu calculated is 3.35 and Cc is 1.1489 (which meets the gradation requirements for SW (1<Cc>3 for SW). Therefore, the soil is classified as **a mixture of well graded-sand and clayey sand (SW-SC).**

### 3.13.3 AASHTO classification system

The AASHTO Soil Classification System was developed by the American Association of State Highway and Transportation Officials, and is used as a guide for the classification of

soils and soil-aggregate mixtures for highway construction purposes. Besides Soil Classification on other criteria, the AASHTO Soil Classification System classifies soils into seven primary groups, named A-1 through A-7, based on their relative expected quality for road embankments, sub-grades, sub-bases, and bases. To determine a soil's classification in the AASHTO system, one first determines the relative proportions of gravel, coarse sand, fine sand, and silt-clay using sieve analysis. Granular materials are classified into groups A-1 through A-3. Soils having more than 35% passing the No. 200 sieve are silt-clay and fall in groups A-4 through A-7. Having the proportions of the components and the plasticity data, one enters one of the two alternatives AASHTO classification tables and checks from left to right until a classification is found for which the soil meets the criteria. It should be noted that, in this scheme, group A-3 is checked before A-2. Soils classified as A-1 are typically well-graded mixtures of gravel, coarse sand, and fine sand. Soils in subgroup A-1-a contain more gravel whereas those in A-1-b contain more sand. Soils in group A-3 are typically fine sands that may contain small amounts of non-plastic silt. Group A-2 contains a wide variety of "borderline" granular materials that do not meet the criteria for groups A-1 or A-3. Soils in group A-4 are silty soils, whereas those in group A-5 are high-plasticity elastic silt. Soils in group A-6 are typically lean clays, and those in group A-7 are typically highly plastic clays.

Fine-grained soils are further rated for their suitability for highways by the group index (GI) method, determined as follows:

$$GI = (F - 35)[0.2 + 0.005 (w_L - 40)] + 0.01 ( F - 15)(I_P-10)$$

Where, F = percentage by mass passing through the No. 200 sieve (0.075 mm sieve) expressed as a whole number.

$w_L$ = Liquid Limit of the soil(%) expressed as a whole number

$I_P$= Plasticity Index of the soil(%) expressed as a whole number

The Group Index value generally ranges between 0 and 20. The smaller the value of the group index, the better is the soil in that category. A group index of zero indicates a good subgrade, whereas a group index of 20 or greater shows a very poor subgrade. The Group Index value is zero for granular materials (sand, gravel). Therefore, these are better soils to be used as subgrade materials.

The soil samples collected from the three respective locations(locations 1, 2 and 3) is classified using AASHTO classification system and a general rating to be used as subgrade material is given.

(i) Location 1- Pallathuruthy, Alappuzha

The soil sample consists of granular materials, since less than 35% particles is passing through 0.075 mm IS sieve (1.1%). Therefore, the soil would be classified under either A-1, A-2 or A-3 types. The percentage of soil particles passing 2.00 mm IS sieve is 85.1%. The percentage of soil particles passing 0.425 mm IS sieve is 36.7% (50 max) and the percentage of soil particles passing 0.075 mm IS sieve is 1.1% (25 max). Therefore, the soil can be classified under **A-1-b** type. The soil with the lowest number, A-1 is the most suitable as a highway material or subgrade. A-1-b type soil consists predominantly of coarse sand. The group index value is zero. Therefore, these are better soils to be used as subgrade materials.

(ii) Location 2- Kainakary, Alappuzha

The soil sample consists of silt-clay materials, since more than 35% particles is passing through 0.075 mm IS sieve (58.2%). Therefore, the soil would be classified under either A-4, A-5, A-6 or A-7 types. The liquid limit of the soil is 34.5% (40 max) and plasticity index is 14.86 (11 max).Therefore, the soil can be classified under A-6 type. The usual types of significant constituent materials in this type of soil include clayey particles. These are usually plastic clays, having values of plasticity index exceeding 10% and low values of liquid limit below 40%; they have high volume change properties with variation in moisture content. A-6 type soil is generally rated as fair to poor type soil for use as a subgrade material.

Since, the soil is fine-grained, this type of soil can be further classified using Group Index.

Here, F= 58.2 ~ 58, $w_L$ = 34.5 ~ 35 and $I_P$ = 14.86 ~ 15,

$$GI = (F - 35)\,[0.2 + 0.005\,(w_L - 40)] + 0.01\,(F - 15)(I_P - 10)$$

$$= (58 - 35)\,[0.2 + 0.005\,(35 - 40)] + 0.01\,(58 - 15)(15 - 10)$$

$$= 6.175, \text{ say } 6.$$

Therefore, the soil is designated as **A-6 (6).**

(iii) Location 3- Mampuzhakary, AC road

The soil sample consists of granular materials, since less than 35% particles is passing through 0.075 mm IS sieve (7.8%). Therefore, the soil would be classified under either A-1, A-2 or A-3 types. The percentage of soil particles passing 2.00 mm IS sieve is 89.75%. The percentage of soil particles passing 0.425 mm IS sieve is 69.2% (51 min) and the percentage of soil particles passing 0.075 mm IS sieve is 7.8% (10 max). Therefore, the soil can be classified under **A-3** type. These soils consists mainly, uniformly graded medium or fine sand. The group index value is zero. Therefore, these are better soils to be used as subgrade materials.

### 3.13.4 Summary of soil classification

The soil sample collected from Kainakary, Alappuzha was found to have a group index value of 6 and by the AASHTO soil classification system, the soil should be rated as a poor material for subgrade. Therefore, the soil constituting this location is identified as the weak soil amongst the three and collected and analysed for further study.

## 3.14 DATA COLLECTION AND MATERIAL COLLECTION

The soil sample identified as the poor material for subgrade is found to constitute the subgrade for majority of the roads in Kainakary, Alappuzha. Therefore, this soil is procured in much higher quantity for further tests. The site chosen for study is located adjacent to the starting of Alappuzha-Changanassery road section. The location from where the soil was procured is shown in figure 3.24. The top soil was removed and soil at a depth of 10 cm from the top was procured. Almost 35 kg of soil was collected in each of the two rounds of site visits.

Figure 3. 24 Location of the road (adjacent to the A-C road section), from where soil is procured in Kainakary, Alappuzha

The present data of the road which is located at the starting of A-C road section was collected from the Office of the Assistant Engineer, PWD roads division, Alappuzha (table 3.10). The existing road is estimated to carry a traffic of 2,897,935 ESAL applications (2.89 msa) as per PWD records.

Table 3. 10 Existing data of the road section collected from Office of the Assistant Engineer, PWD roads division, Alappuzha

| **Layers of flexible pavement** | **Layer thickness (mm)** | **Elastic modulus (Mpa)** | **Poisson's ratio** |
|---|---|---|---|
| DBM | 120 mm | 2512 Mpa | 0.35 |
| GB | 100 mm | Estimated | 0.35 |
| GSB | 200 mm | Estimated | 0.35 |
| Subgrade | ___ | Estimated | 0.35 |

Natural and synthetic geotextiles are used as geosynthetics which are used as part of subgrade improvement or stabilization. The natural geotextile procured was coir geotextile which was chosen since it is economic and readily available in Alappuzha district (figure 3.25). The synthetic geotextile procured was non-woven polyester geotextile, which was chosen since it performs better in drainage, separation and filtration (figure 3.26). 8 square metre of both the materials was procured in quantity. The geotextiles were placed at a depth of H/4 from top and H/4 from bottom of the CBR mould.

Figure 3. 25 Coir mat (Coir geotextile)

Figure 3. 26 Polyester geotextile

## 3.15 TEST RESULTS

The most common laboratory test for soil compaction is the Proctor compaction test. In addition, the soil is compacted in 5 layers with 25 blows per layer. The test is conducted for 5 moisture contents to obtain the optimum water content ($w_{opt}$), for which the value of the dry unit weight is maximum ($\gamma_{d,max}$). The results of the compaction test is shown in table 3.11 and the compaction curve plot is shown in figure 3.27.

Empty weight of mould ($W_1$) = 4.627 kg

Diameter of mould (d) = 10 cm

Height of mould (h) = 12.6 cm

Therefore, volume of mould = $\frac{\pi}{4} * d^2 * h$

= 1000 $cm^3$

Table 3. 11 Result of compaction test performed

| Sl. No. | Weight of mould + compacted soil ( $W_2$) | Water content ( w % ) | Weight of compacted soil ( $W_2 - W_1$) | Wet density ($\gamma$) in $g/cm^3$ | Dry density ( $\gamma_d = \frac{\gamma}{1+w}$ ) in $g/cm^3$ |
|---|---|---|---|---|---|
| 1 | 6.707 | 10 | 2.079 | 2.079 | 1.89 |
| 2 | 6.936 | 16 | 2.308 | 2.308 | 1.99 |
| 3 | 7.115 | 19 | 2.487 | 2.487 | 2.089 |
| 4 | 7.118 | 22 | 2.49 | 2.49 | 2.04 |
| 5 | 7.003 | 25 | 2.375 | 2.375 | 1.9 |

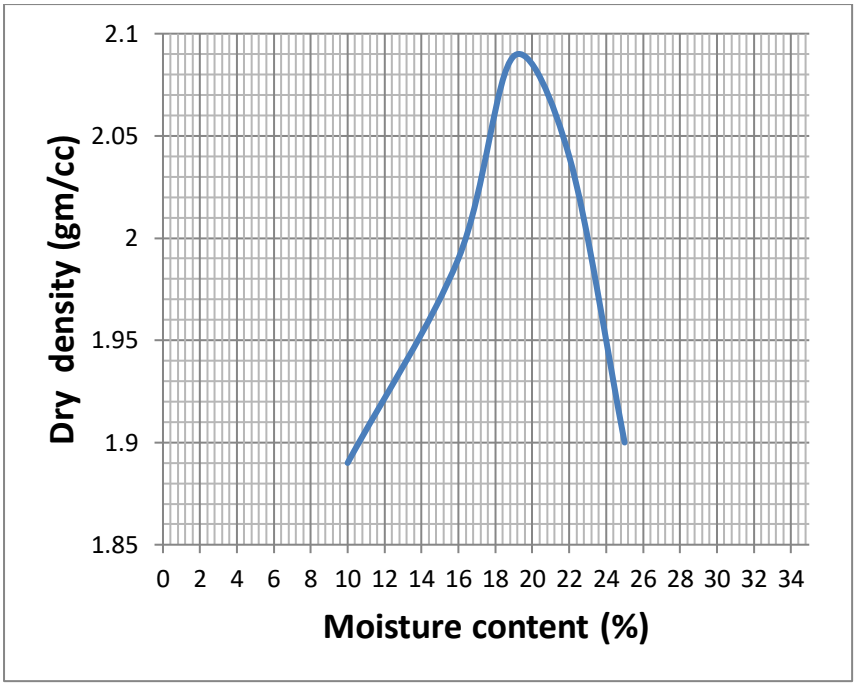


Figure 3. 27 Compaction curve

From graph, maximum dry density is obtained at 2.089 g/cm$^3$ and water content corresponding to it is 19.2%.

The California Bearing Ratio test is penetration test meant for the evaluation of subgrade strength of roads and pavements. The results obtained by these tests are used with the empirical curves to determine the thickness of pavement and its component layers. This is the most widely used method for the design of flexible pavement. California Bearing Ratio (CBR) is the ratio of force per unit area required to penetrate a soil mass with standard circular piston at the rate of 1.25 mm/min. to that required for the corresponding penetration of a standard material.

$$\text{C.B.R.} = \frac{\text{Test load}}{\text{Standard load}} \times 100$$

For the optimum moisture content equal to 19.2 %, CBR tests were performed on the soil. The geotextiles (coir and non-woven polyester) were placed at a depth of H/4 from top and H/4 from bottom of the CBR mould. Figure 3.28 shows the CBR mould with geotextile being kept in position. 20 CBR tests were performed in total for 4 conditions ie., Unsoaked condition, soaked condition for 4 days of submergence, soaked condition for 7 days of submergence and soaked condition for 14 days of submergence. Figure 3.29 shows the

picture of soaked CBR test performed for 7 days of submergence. The results of CBR tests are shown in table 3.12.

Figure 3. 28 CBR mould with geotextile being kept in position

Figure 3. 29 Soaked CBR mould

Table 3. 12 Result of CBR tests performed (reported in %)

| CONDITION | Conventional | Natural Geotextile at h/4 from bottom | Natural Geotextile at h/4 from top | Synthetic Geotextile at h/4 from bottom | Synthetic Geotextile at h/4 from top |
|---|---|---|---|---|---|
| Unsoaked | 3.71 | 4.98 | 5.12 | 5.85 | 6 |
| 4-day soaked | 2.93 | 3.83 | 4.18 | 4.92 | 4.67 |
| 7-day soaked | 1.51 | 1.94 | 2 | 2.75 | 2.63 |
| 14-day soaked | 1.76 | 2.08 | 2.26 | 2.88 | 3.04 |

The CBR values when the geotextiles were placed at h/4 from top is observed to be higher than those when placed at h/4 from bottom except the 4-day and 7-day soaked conditions of the synthetic geotextile. The conventional CBR value of the soil is reported as 3.71%. By proper geosynthetic materials, the CBR values were improved from 3.71% to 6%. The maximum CBR value is reported as 6% corresponding to that of the synthetic geotextile (non-woven polyester), placed at h/4 from top. The CBR values were observed to decrease for the soaked conditions. The decrease in CBR value was from 3.71% to 2.93% when the period of submergence is 4 days, 3.71% to 1.51% when the period of submergence is 7 days and 3.71% to 1.76% when the period of submergence is 14 days. There is a small increase in CBR value from 1.51% to 1.71% because of the thixotropic nature of clayey soil due to which the soils starts to regain its strength. Stabilization has resulted in an increase in CBR value by about 25% and 50% from the conventional cases.

### 3.15.1 Results of resilient modulus of subgrade and granular layers ($M_{RS}$ and $M_{RGRAN}$)

Table 3.13 and table 3.14 shows the calculated results of elastic moduli values for the subgrade and combined granular layer (base and GSB) as per the provisions provided in IRC-37, 2018.

Table 3. 13 Result of resilient modulus of subgrade (in MPa)

| CONDITION | Conventional | Natural Geotextile at h/4 from bottom | Natural Geotextile at h/4 from top | Synthetic Geotextile at h/4 from bottom | Synthetic Geotextile at h/4 from top |
|---|---|---|---|---|---|
| Unsoaked | 37.1 | 49.8 | 50.05 | 54.51 | 55.40 |
| 4-day soaked | 29.3 | 38.3 | 41.8 | 49.2 | 46.7 |
| 7-day soaked | 15.1 | 19.4 | 20 | 27.5 | 26.3 |
| 14-day soaked | 17.6 | 20.8 | 22.6 | 28.8 | 30.4 |

Table 3. 14 Result of resilient modulus of combined granular layer (in MPa)

| CONDITION | Conventional | Natural Geotextile at h/4 from bottom | Natural Geotextile at h/4 from top | Synthetic Geotextile at h/4 from bottom | Synthetic Geotextile at h/4 from top |
|---|---|---|---|---|---|
| Unsoaked | 96.63 | 129.71 | 130.37 | 141.98 | 144.29 |
| 4-day soaked | 76.31 | 99.75 | 108.87 | 128.14 | 121.63 |
| 7-day soaked | 39.33 | 50.53 | 52.09 | 71.62 | 68.49 |
| 14-day soaked | 45.84 | 54.17 | 58.86 | 75.01 | 79.17 |

# CHAPTER 4

# RESULTS AND DISCUSSIONS

## 4.1 RESPONSE ANALYSIS USING IITPAVE AND KENPAVE

### 4.1.1 Variation of mechanistic-empirical parameters over change in elastic moduli of subgrade and granular layers

The elastic moduli associated with the change in CBR values which are calculated as shown in tables 3.15 and 3.16 are used to estimate various mechanistic empirical parameters of the pavement for the existing layer thicknesses (120 mm DBM and 300 mm Granular layer). The vertical compressive strain and horizontal tensile strains calculated for constant layer thicknesses were represented in a set of graphs to better understand the trends in the variation of values as shown in the Figure 4.1 and Figure 4.2. Similarly,the rutting life and fatigue life were plotted as shown in Figure 4.3 and 4.4 respectively. The results obtained from KENPAVE and IITPAVE were similar and followed the same trend.

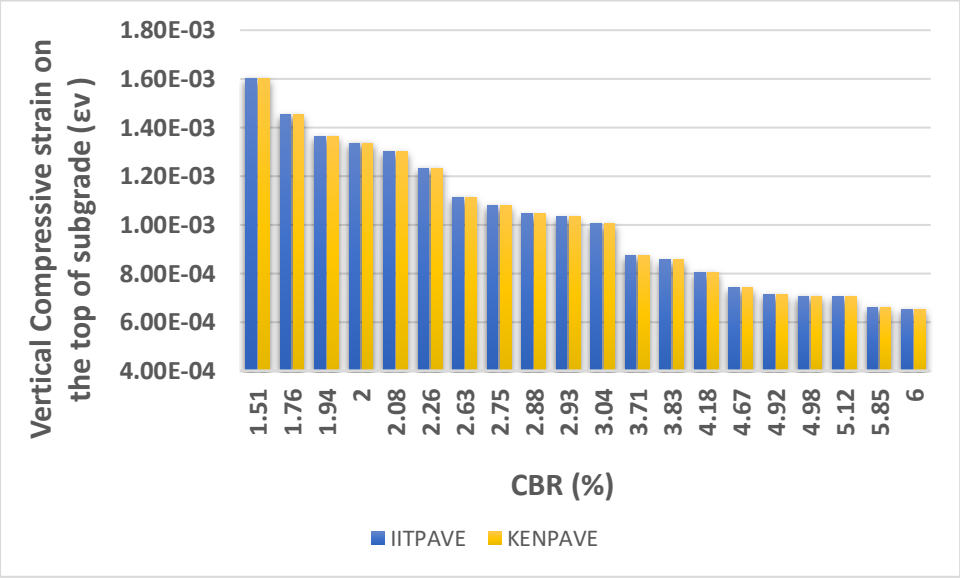


Figure 4. 1 Variation of vertical compressive strain on the top of subgrade with CBR of subgrade and elastic moduli of subgrade and granular layers

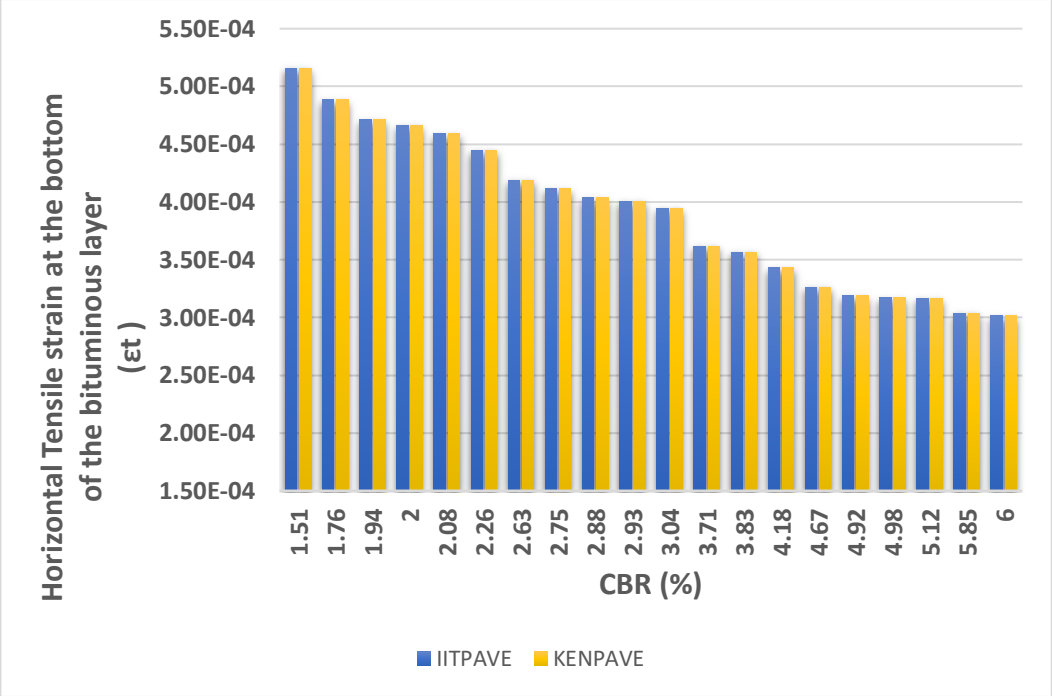


Figure 4. 2 Variation of horizontal tensile strain at the bottom of bituminous layer with CBR of subgrade and elastic moduli of subgrade and granular layers

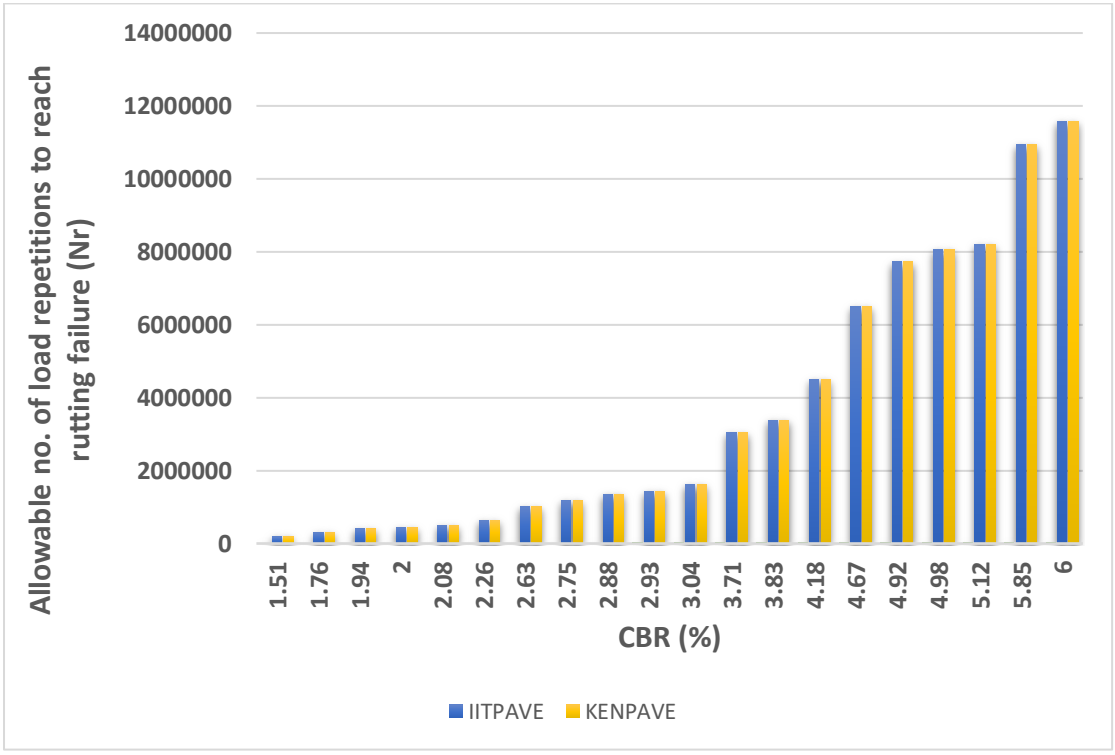


Figure 4. 3 Variation of estimated rutting life with CBR of subgrade and elastic moduli of subgrade and granular layers

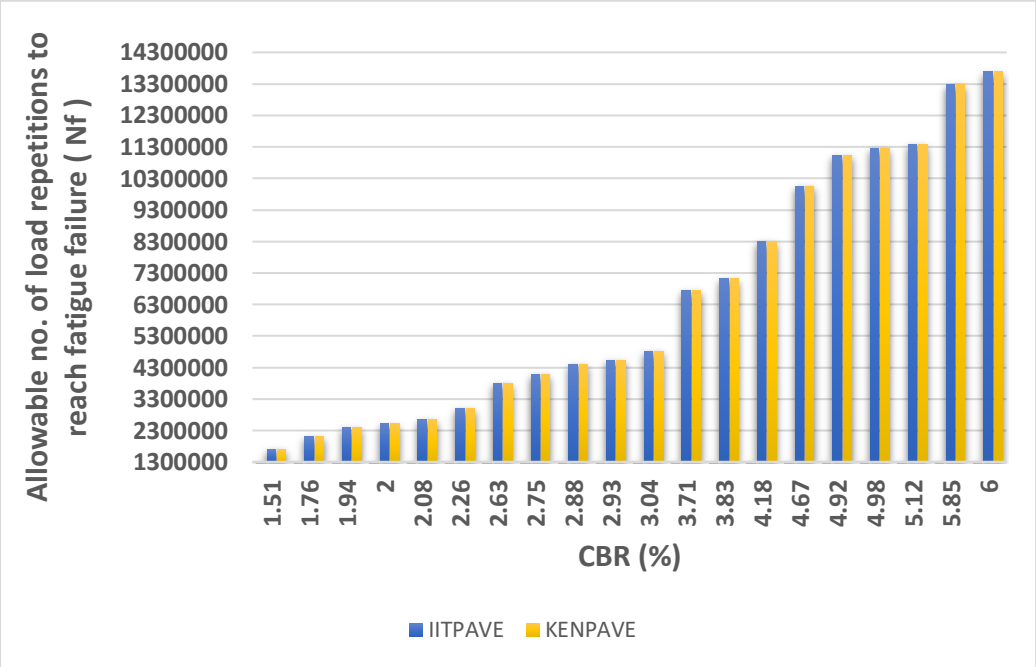


Figure 4. 4 Variation of estimated fatigue life with CBR of subgrade and elastic moduli of subgrade and granular layers

As the CBR of subgrade increases, the elastic moduli of the subgrade and the granular layer increases, the mechanistic parameters like vertical compressive strain and horizontal tensile strain decreases, thereby increase in rutting life and fatigue life respectively.

### 4.1.2 Variation of mechanistic-empirical parameters over change in thickness of pavement layers

The vertical compressive strain and horizontal tensile strains calculated for different combinations of layer thicknesses (table 3.1) and for constant elastic moduli of subgrade corresponding to conventional CBR of 3.71 ($M_{RS}$ = 37.1 MPa) were represented in a set of graphs to better understand the trends in the variation of values as shown in the Figure 4.5 and Figure 4.6. The elastic modulus of granular layers are affected by the thickness of the granular layer (equation 3.3). Therefore, along with the variation in thickness of granular layer, the elastic modulus of granular layer was also varied.

Similarly, the rutting life and fatigue life were plotted as shown in Figure 4.7 and 4.8 respectively. The results obtained from KENPAVE and IITPAVE were similar and followed the same trend.

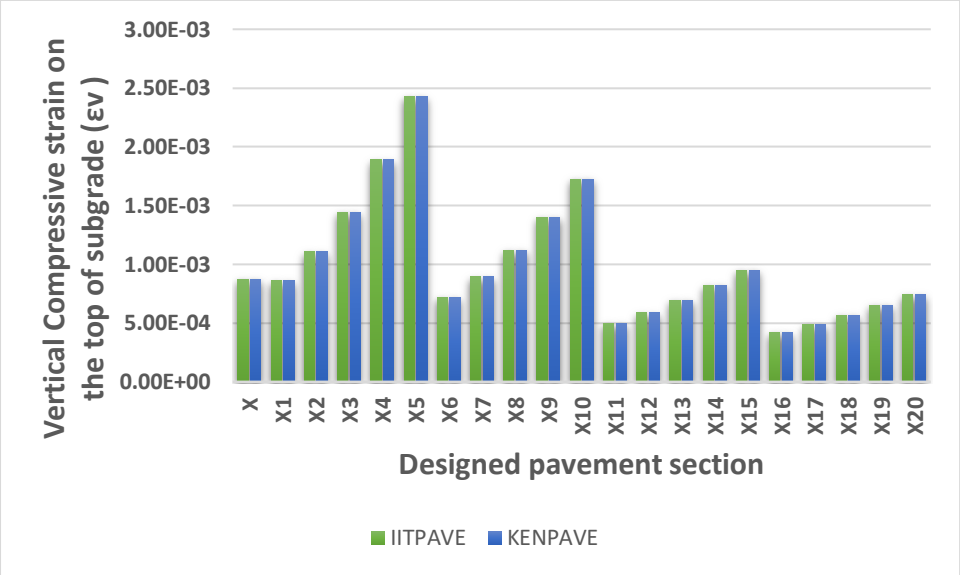


Figure 4. 5 Variation of compressive strain on subgrade with designed pavement sections

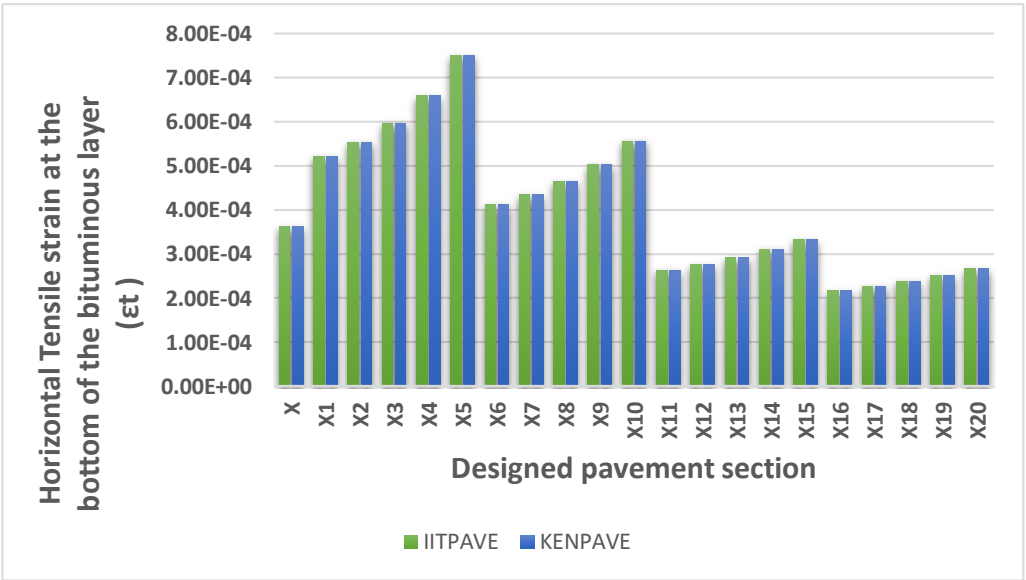


Figure 4. 6 Variation of tensile strain at the bottom of bituminous layer with designed pavement sections

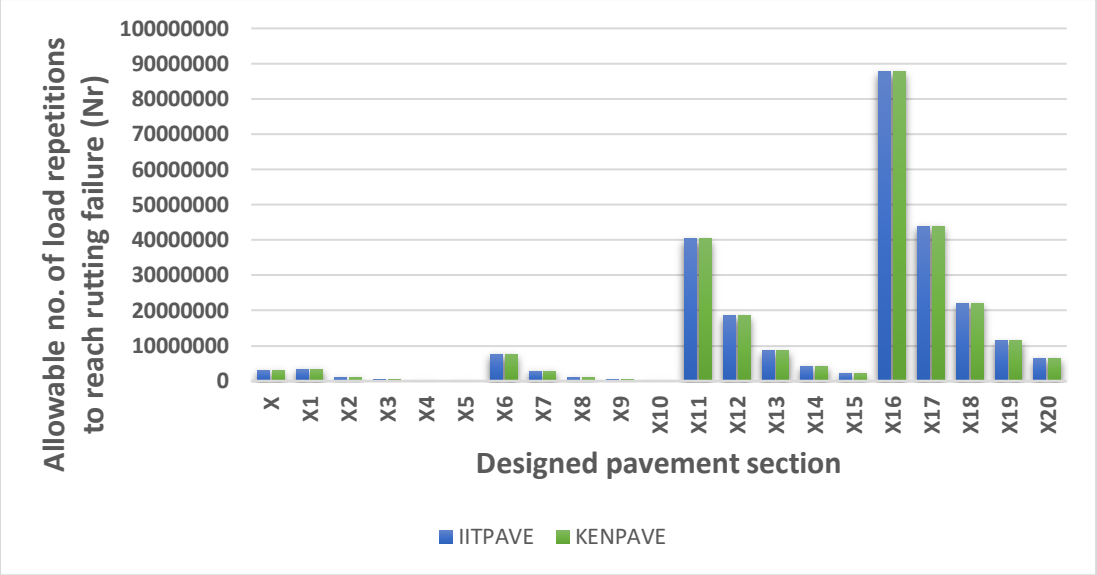


Figure 4. 7 Variation of estimated rutting life with designed pavement sections

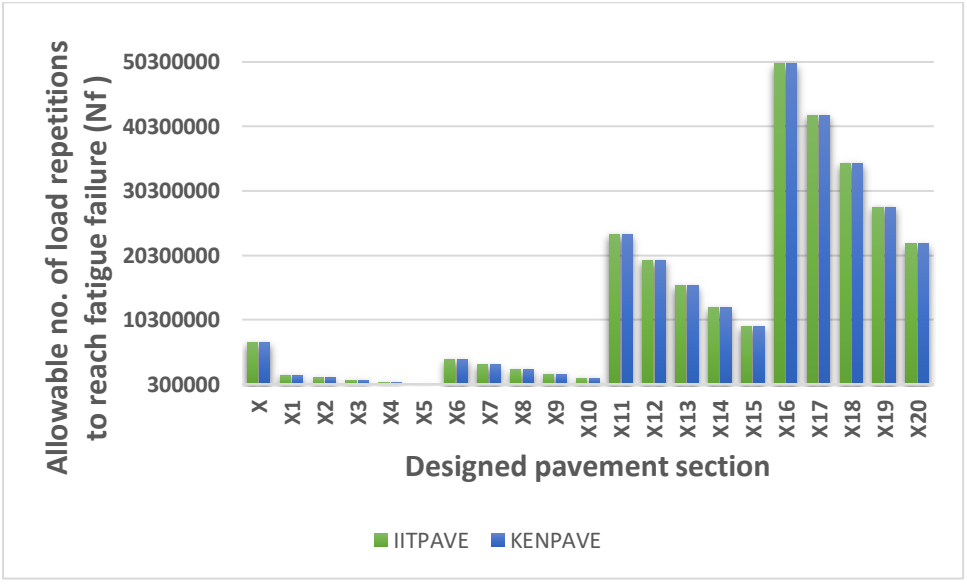


Figure 4. 8 Variation of estimated fatigue life with designed pavement sections

The lower value of vertical compressive strain on the top of subgrade and the horizontal tensile strain was observed in the section 16. Therefore the rutting life and fatigue life of the section 16 found be higher value. As the thickness of the bituminous layer and the granular layer increases the mechanistic parameters like vertical compressive strain and horizontal tensile strain decreases, thereby increase in rutting life and fatigue life respectively. But the selection of a pavement section should consider the economic aspect.The tensile strain under the bituminous layer is observed to vary non-linearly with the change in thickness of the bituminous layer.

This trend has a peculiar nature. The tensile strain increases with increase in the thickness of bituminous layer up to a critical thickness and then starts decreasing with further increase in thickness. This trend can be seen in Figure 4.10 for different thicknesses of the granular layer (sub-base and base combined). The reason attributed to this behaviour is how the bituminous layer distributes the loads on to the granular layer in the case of thick bituminous layers. If the flexural rigidity of the bituminous layer is high (in the form of thickness and/or bituminous layer's modulus) compared to that of the granular layer, the load distribution will be done predominantly by the bituminous layer and hence may lead to higher tensile strains.

The variation of compressive strain on top of the subgrade with the thickness of bituminous layer follows a uniform trend. The compressive strain decreases with increase in the thickness of the bituminous layer as shown in Figure 4.9. The compressive strain on top of subgrade decreases with increase in bituminous layer thickness and also with the increase in the granular layer thickness. However, the effect of an increase in the thickness of the bituminous layer is less for a higher thickness of the granular layer as can be seen in Figure 4.9. This can be attributed to the ability of a thick granular layer in distributing the vertical load before transmitting them onto the subgrade soil. Though the granular layers cannot be considered for carrying tensile loads, their ability to distribute the load through compression is very effective with aggregate interlocking aiding in the increase of the area of load distribution on the subgrade. The effect of bituminous layer thickness on compressive strain on subgrade decreases with increase in the thickness of the granular layer. The number of repetitions to reach rutting failure or fatigue failure of the pavement can be estimated from the value of vertical compressive strain on top of subgrade and the tensile strain at the bottom of bituminous layer using equations 3.4 and 3.6 as discussed earlier. Figure 4.11 shows the variation of rutting life with a thickness of the bituminous layer, and it shows a fairly uniform trend of increase in rutting life with an increase in the thickness of bituminous layer for all the granular layer thicknesses considered in the study. The estimated fatigue life values (in number) for different bituminous layer and granular layer thicknesses are presented in the graph shown in Figure 4.12. This graph indicates a constant variation in fatigue life when the bituminous layer thickness is increased from 50 mm to 100 mm as there is a shift

in the load distribution mechanism between the thickness values of 50 mm and 100 mm. Figure 4.11 and 4.12 also shows the degree of variation in the rutting life and fatigue life with an increase in the thickness of the granular layer and bituminous layer.

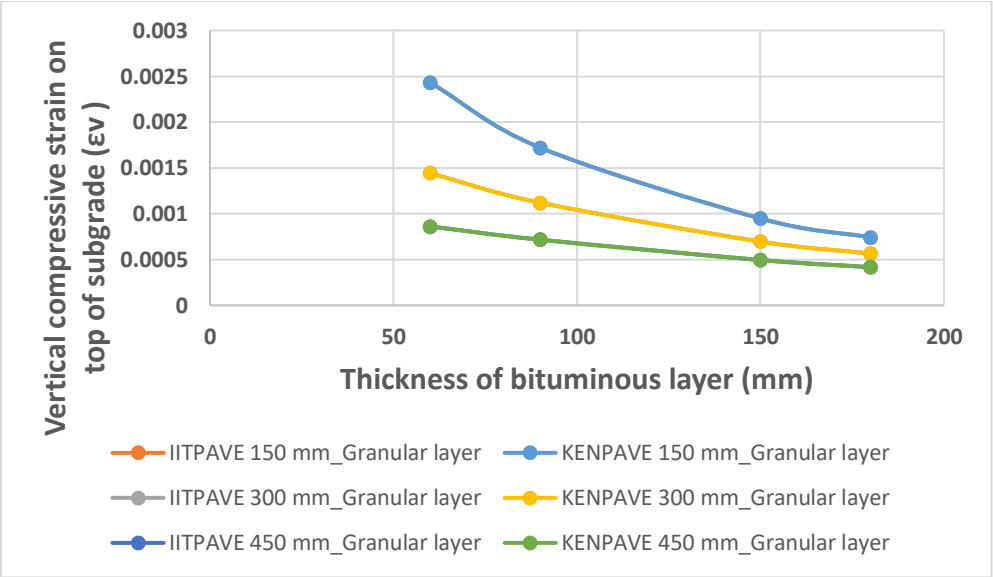


Figure 4. 9 Variation of compressive strain on subgrade with the thickness of the bituminous layer

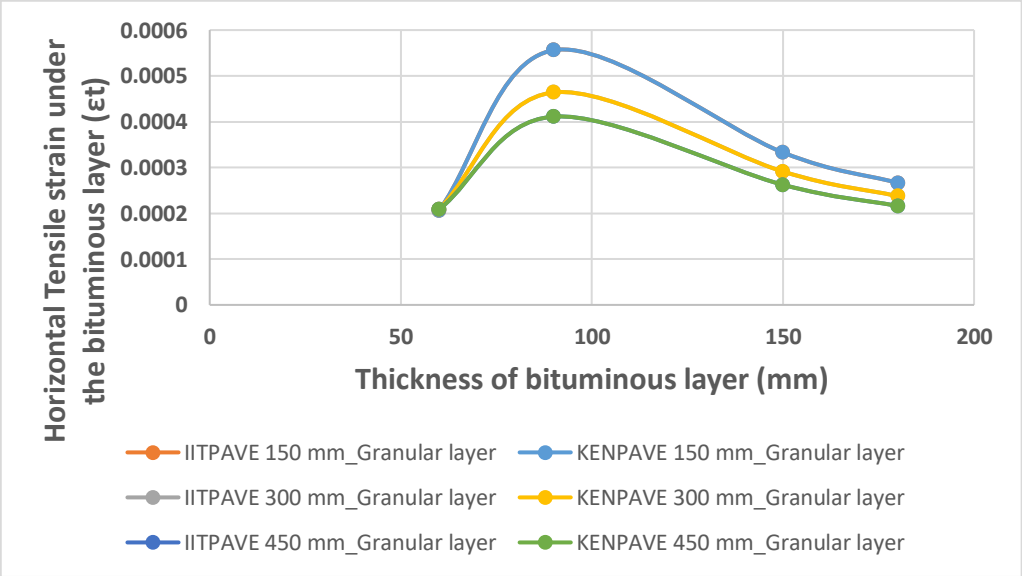


Figure 4. 10 Variation of horizontal tensile strain under the bituminous layer with the thickness of the bituminous layer

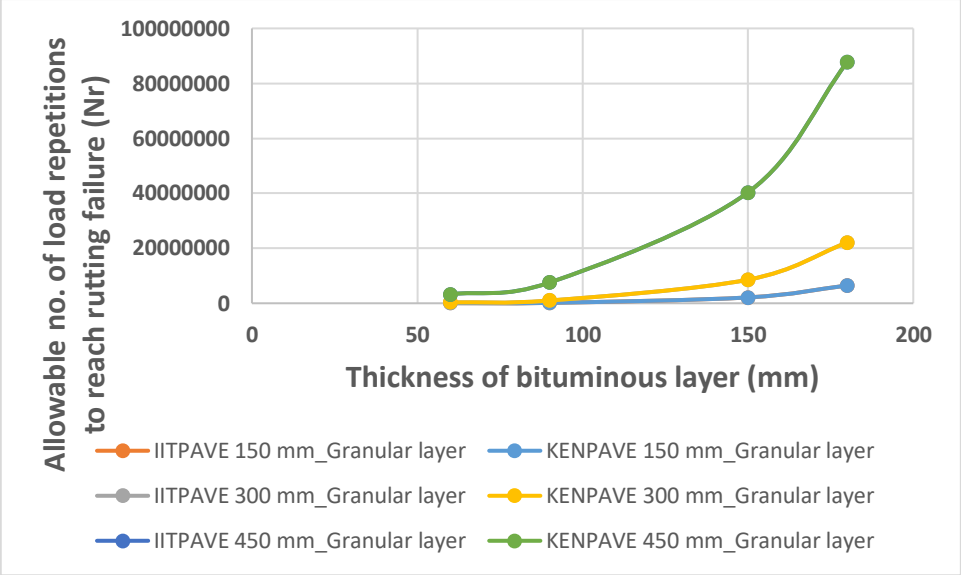


Figure 4. 11 Variation of estimated rutting life with the thickness of the bituminous layer

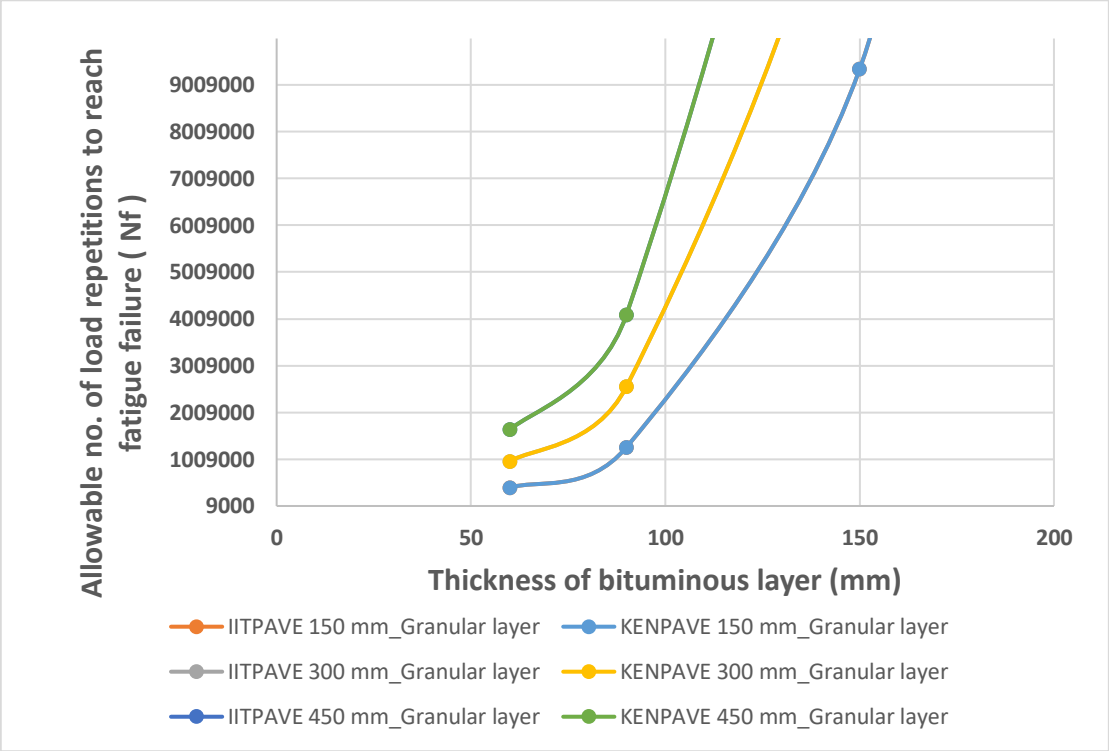


Figure 4. 12 Variation of estimated fatigue life with the thickness of the bituminous layer

### 4.1.3 Variation of mechanistic-empirical parameters over period of submergence of subgrade

The variation of mechanistic empirical parameters like vertical compressive strain at the top of subgrade, horizontal tensile strain at the bottom of bituminous layer, deflection at the bottom of bituminous layer, estimated rutting life and fatigue life of

the pavement are studied for the linear elastic condition in IITPAVE software. Though the pavement surface deflection is not considered in the design, it gives a good indication of the pavement structure's ability to distribute the load. AASHO road tests and the AASHTO's pavement design guidelines are based on the pavement surface deflection measurements made with Benkelman beam. The pavement has deflected more for the seven day submerged condition of the subgrade (by about 0.18 mm) as shown in figure 4.13. The benefit of using proper subgrade material and thereby improving the elastic moduli values of the subgrade and granular layers was reflected in the study. When the subgrade was submerged for longer periods, the mechanistic empirical parameters like vertical compressive strain at the top of subgrade and the horizontal tensile strain at the bottom of bituminous layer were found to increase considerably (figures 4.14 and 4.15), thereby a decrease in the fatigue and rutting lives of the pavement was observed as shown in figures 4.16 and 4.17. The effect of using coir geotextile (natural) and non-woven polyester geotextile (synthetic) has improved the mechanistic parameters like rutting life and fatigue life from the conventional scenarios. Geosynthetics placed at h/4 from top was found to outperform in mechanistic parameters than geosynthetics placed at h/4 from bottom. When the subgrade was submerged for 7 days and 14 days, adequate geosynthetics like polyester synthetic had increased the values of rutting and fatigue life from its conventional cases and had almost brought back the estimated rutting and fatigue life values to the 4-day soaked conventional condition.

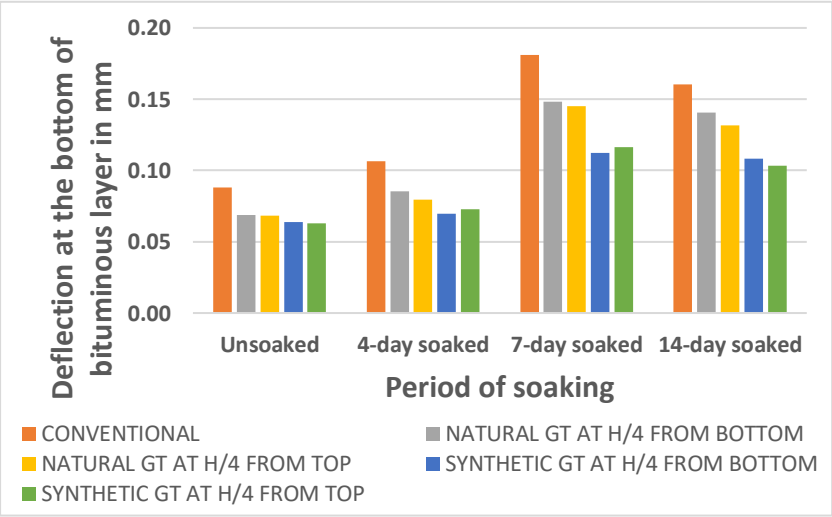


Figure 4. 13 Variation of deflection at the bottom of bituminous layer over period of submergence of subgrade for linear-elastic condition

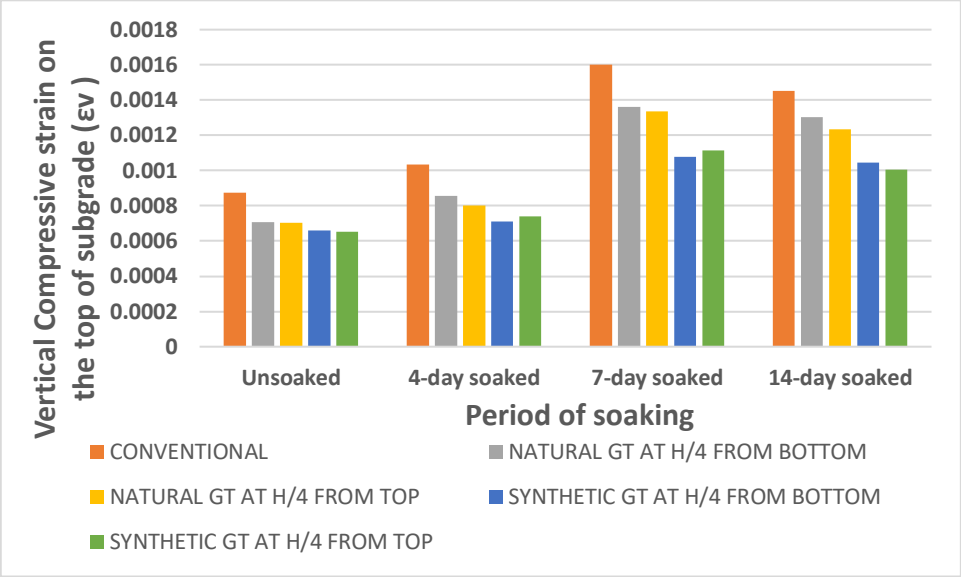


Figure 4. 14 Variation of vertical compressive strain on the top of subgrade over period of submergence of subgrade for linear-elastic condition

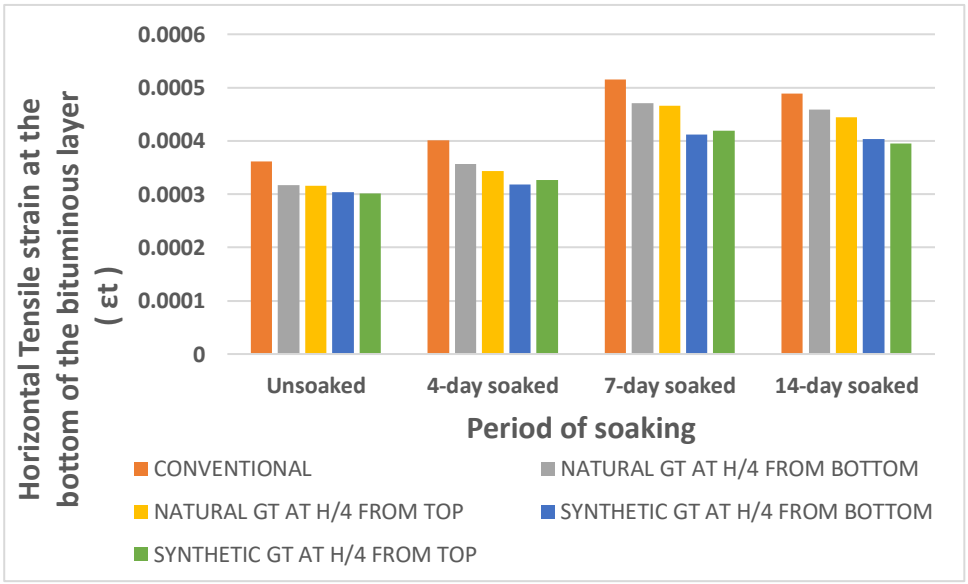


Figure 4. 15 Variation of horizontal tensile strain at the bottom of bituminous layer over period of submergence of subgrade for linear-elastic condition

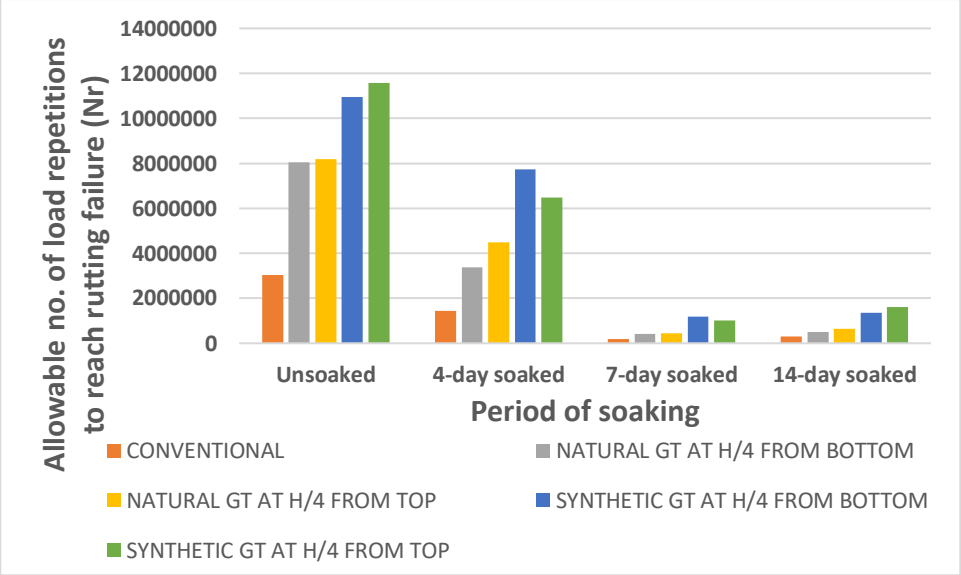


Figure 4. 16 Variation of estimated rutting life over period of submergence of subgrade for linear-elastic condition

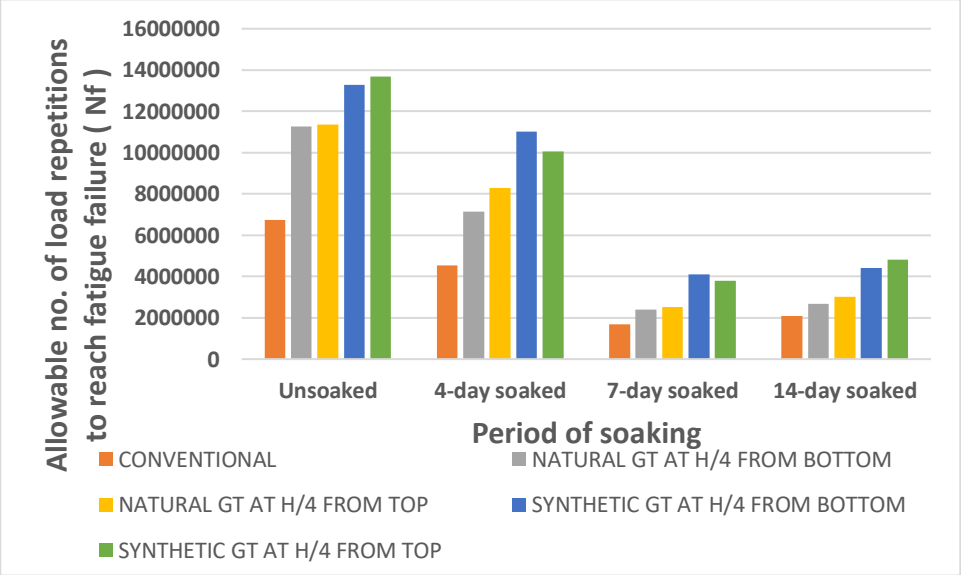


Figure 4. 17 Variation of estimated fatigue life over period of submergence of subgrade for linear-elastic condition

## 4.2 DAMAGE ANALYSIS USING KENPAVE

For damage analysis, fatigue coefficients are noted as FT1, FT2 and FT3, and the values are 0.0796, 3.291 & 0.854 respectively. Similarly permanent deformation coefficients FT4 = 1.365E-09 and FT5 = 4.477. The volume of traffic is 2, 897, 935 ESAL applications (2.89 msa). The output page of KENLAYER programme performed for damage analysis is shown in figure 4.18. Damage analysis was performed and the damage ratio was observed for two cases ie., damage ratio over change in elastic moduli of subgrade and granular layers(figure 4.19) and damage ratio over change in thickness of pavement layers (figure 4.20). The elastic modulus of granular layers are affected by the thickness of the granular layer (equation 3.3). Therefore, along with the variation in thickness of granular layer, the elastic modulus of granular layer was also varied.

```
NUMBER OF LAYERS FOR BOTTOM TENSION (NLBT)---- =  1
NUMBER OF LAYERS FOR TOP COMPRESSION (NLTC)--- =  1
LAYER NO. FOR BOTTOM TENSION (LNBT) ARE: 1
LAYER NO. FOR TOP COMPRESSION (LNTC) ARE: 3

LOAD REPETITIONS (TNLR) IN PERIOD 1  FOR EACH LOAD GROUP ARE : 2897935

DAMAGE COEF.'S (FT) FOR BOTTOM TENSION OF LAYER 1  ARE: 0.0796  3.291  0.854

DAMAGE COEFICIENTS (FT) FOR TOP COMPRESSION OF LAYER 3  ARE:  1.365E-09 4.477

DAMAGE ANALYSIS OF PERIOD NO.  1  LOAD GROUP NO.  1

 POINT    VERTICAL   VERTICAL   VERTICAL     MAJOR       MINOR  INTERMEDIATE
                                           PRINCIPAL    PRINCIAL  P. STRESS
  NO.    COORDINATE    DISP.     STRESS      STRESS      STRESS  (HORIZONTAL
                                (STRAIN)    (STRAIN)    (STRAIN)  P. STRAIN)
  1      12.00000    0.06111     123.205     123.533    -995.065    -802.498
          (STRAIN)              2.995E-04   2.996E-04  -3.015E-04  -3.015E-04
  1      42.00010    0.04644      32.351      33.323      -2.321      -0.785
          (STRAIN)              5.974E-04   6.211E-04  -2.475E-04  -2.475E-04

  2      12.00000    0.06294     106.042     106.042    -841.057    -366.876
          (STRAIN)              2.105E-04   2.105E-04  -2.985E-04  -2.985E-04
  2      42.00010    0.04809      35.056      35.056      -2.495      -0.542
          (STRAIN)              6.519E-04   6.519E-04  -2.631E-04  -2.631E-04

  3      12.00000    0.06111     123.205     123.533    -995.065    -802.498
          (STRAIN)              2.995E-04   2.996E-04  -3.015E-04  -3.015E-04
  3      42.00010    0.04644      32.351      33.323      -2.321      -0.785
          (STRAIN)              5.974E-04   6.211E-04  -2.475E-04  -2.475E-04

AT BOTTOM OF LAYER  1   TENSILE STRAIN =  -3.015E-04
ALLOWABLE LOAD REPETITIONS =   1.052E+05  DAMAGE RATIO =   2.756E+01

AT TOP OF LAYER  3   COMPRESSIVE STRAIN =   6.519E-04
ALLOWABLE LOAD REPETITIONS =   2.500E+05  DAMAGE RATIO =   1.159E+01

******************************
* SUMMARY OF DAMAGE ANALYSIS *
******************************
AT BOTTOM OF LAYER  1     SUM OF DAMAGE RATIO = 2.756E+01
AT TOP OF LAYER  3        SUM OF DAMAGE RATIO = 1.159E+01

MAXIMUM DAMAGE RATO =   2.756E+01   DESIGN LIFE IN YEARS = .04
```

Figure 4. 18 Output page of damage analysis performed in KENPAVE

The reduction in damage ratio is remarkable in the case of stabilized soil. The increase of the CBR of the subgrade associated with a drastic increase in the elastic moduli values of the subgrade and granular layers had reduced the damage ratio to

almost 50%. The damage ratio associated with the conventional CBR of 3.71 is observed to be 50.13 and a modified CBR of 6 had drastically reduced the damage ratio to 27.56 as shown in figure 4.25. Also, the minimum damage ratio is associated with a pavement layer thickness of 180 mm bituminous layer and 450 mm granular layer (X16 pavement section) as shown in figure 4.26. The selection of a pavement section should still be considered based on the economic aspect.

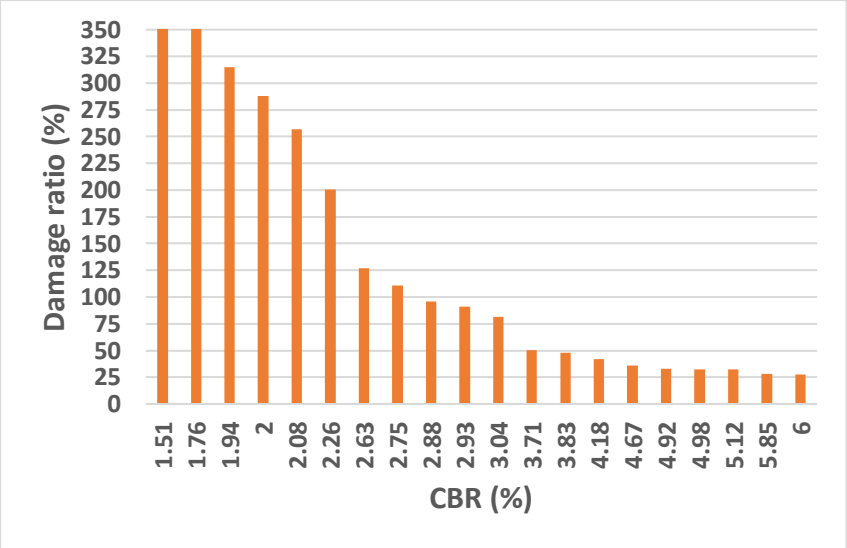


Figure 4. 19 Change in damage ratio over change in CBR and elastic moduli of subgrade and granular layers

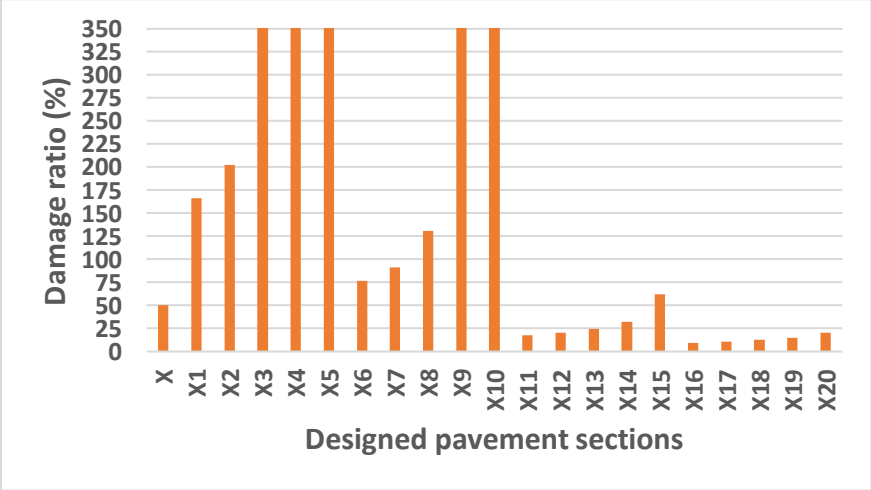


Figure 4. 20 Change in damage ratio over change in thickness of pavement layers designed for conventional CBR and elastic moduli of subgrade

## 4.3 DESIGN OF FLEXIBLE PAVEMENT FOR EFFECTIVE CBR

The existing pavement lacks an embankment and compacted subgrade above it. The CBR of the subgrade soil is improved from 3.71% to 6% through the study. Therefore, the improved CBR is applied in an upper 500 mm selected burrow material and the conventional CBR is provided in the subgrade soil which is provided as embankment below the burrow material.

Elastic modulus of the prepared embankment = 10 * 3.71 = 37.1 MPa

Elastic modulus of the select borrow material (upper 500 mm) = $17.6*(6)^{0.64}$ = 55.40251 MPa

Consider a two-layer elastic system consisting of 500 mm of select borrow soil of modulus 55.40251 MPa and the semi-infinite embankment soil of modulus 37.1 MPa. Consider the Poisson's ratio value of both the layers to be 0.35. Apply a single load of 40,000 N at a contact pressure of 0.56 MPa. Radius of circular contact area for this load and contact pressure = 150.8 mm. Calculate surface deflection at the centre of the load using IIPAVE (no of layers = 2; elastic moduli of 55.4 MPa and 37.1 MPa; Poisson's ratio of 0.35 for both the layers; thickness of 500 mm for upper layer; single wheel load of 40000 N, analysis points = 1; Depth = 0 mm; Radial distance = 0 mm. For this input data, surface deflection = 2.91 mm from IITPAVE.

For an equivalent single layer system, the modulus value of the single layer which will produce the same surface deflection of 2.91 mm for the same load and for a Poisson's ratio of 0.35

$= [2(1-\mu\ 2\ )pa]/\delta$

= [2(1-0.352 )*0.56*150.8]/2.91 = 50.9 MPa

As per these design guidelines, the effective modulus value will be limited to 50 MPa for design purpose. The corresponding CBR (using equation 3.2) is 5.11 % for 105.1 MPa. For a restricted modulus value of 50 MPa, the corresponding effective CBR can be reported as 5 %.

## 4.4 COST COMPARISONS

The layer combinations suitable for a minimum of 2.89 msa traffic, subgrade effective CBR 5%, improved elastic modulus of subgrade and granular layers for effective CBR are highlighted in the table 4.1 for different bituminous layer thicknesses and granular layer thicknesses chosen in the study. The effect of increasing the subgrade CBR and thereby the

elastic moduli of subgrade and granular layers had increased the rutting and fatigue lives of thin bituminous surfaced pavements. The pavement is bound to withstand a traffic of more than 2.89 msa even if the bituminous layer thickness is halved (from existing 120 mm to 60 mm) or reduced to 90 mm. As shown in figure 4.27, the damage ratio associated with the pavement sections designed for effective CBR and improved elastic moduli of pavement layers, were found to be about 50% less than the damage ratio associated with the pavement sections designed for the conventional case (figure 4.21).

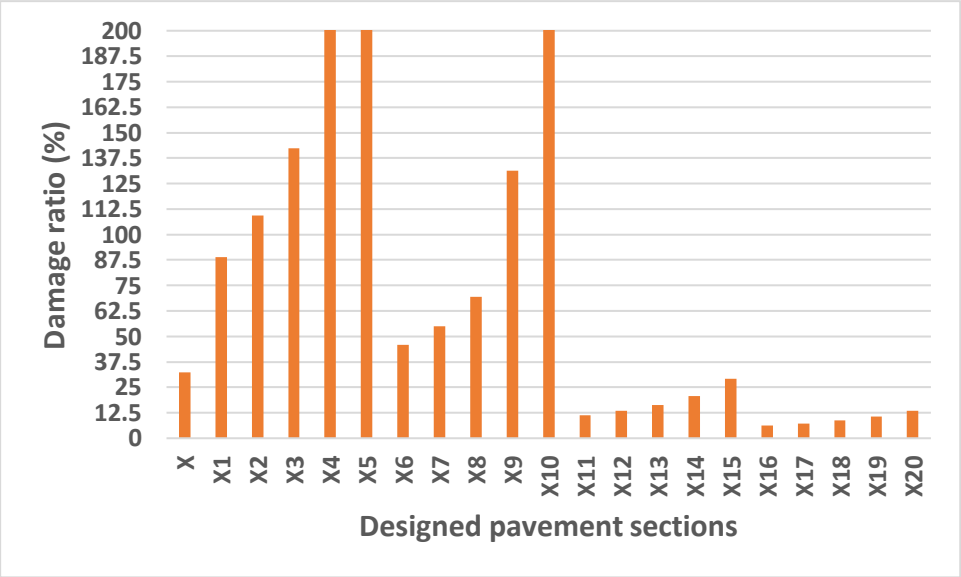


Figure 4. 21 Change in damage ratio over pavement sections designed for effective CBR and improved elastic moduli of subgrade and granular layers

Based on the fatigue life and rutting life of different combinations of the granular layer and bituminous layer thicknesses, some cost comparisons were presented in this section (table 4.2) to highlight the advantages of thin bituminous surface pavements. The cost comparisons and environmental benefits are presented in this section. However, the environmental benefits are not quantified for consideration in the decision-making process.

Table 4.1 Number of load repetitions for fatigue and rutting criterion

| Bituminous layer thickness in mm | Rutting life for 150 mm Granular Layer | Fatigue life for 150mm Granular Layer | Rutting life for 300mm Granular Layer | Fatigue life for 300mm Granular Layer | Rutting life for 450mm Granular Layer | Fatigue life for 450mm Granular Layer |
|---|---|---|---|---|---|---|
| 60 | 8.87E+04 | 759244.83 | 1.04E+06 | 1964759.43 | **1.13E+07** | **3421586.677** |
| 90 | 3.63E+05 | 2135073.54 | **2.93E+06** | **4597985.361** | **2.41E+07** | **7527407.285** |
| 150 | **4.52E+06** | **14157275.9** | **2.14E+07** | **25476259.01** | **1.12E+08** | **39499798.27** |
| 180 | **1.30E+07** | **32190945.42** | **5.19E+07** | **53769042.75** | **2.32E+08** | **80498469.12** |

The cost estimate for the selected layer combinations to withstand 2.89 msa oftraffic is presented in Table 4.2 per 1 m length and 9 m width of the pavement section. So, a typical volume estimate for pavement layers will be length x width x thickness, where length is considered as 1 m and width as 9 m. Hence, the volume of mix required is 9*h,where h is the thickness of the layer in m.

Table 4.2 Cost estimates for the selected alternative pavement compositions

| Combination number | Bituminous Layer thickness (m) | Granular layer thickness (mm) | Cost of bituminous layer (Rs.) | Cost of granular layer (Rs.) | Total cost (Rs.) |
|---|---|---|---|---|---|
| 1 | 0.06 | 0.45 | 5407.18 | 10767.53 | **16174.71** |
| 2 | 0.09 | 0.3 | 8110.77 | 7178.36 | **15289.13** |
| 3 | 0.09 | 0.45 | 8110.77 | 10767.53 | 18878.31 |
| 4 | 0.15 | 0.15 | 13517.95 | 3589.18 | 17107.13 |
| 5 | 0.15 | 0.3 | 13517.95 | 7178.36 | 20696.31 |
| 6 | 0.15 | 0.45 | 13517.95 | 10767.53 | 24285.49 |
| 7 | 0.18 | 0.15 | 16221.55 | 3589.18 | 19810.72 |
| 8 | 0.18 | 0.3 | 16221.55 | 7178.36 | 20696.31 |
| 9 | 0.18 | 0.45 | 16221.55 | 10767.53 | 26989.08 |

The alternatives 1 and 2, known as thin bituminous surfacing is found to have around 33% saving of cost compared to alternative 9. The alternative 1, though the thickness

of the granular layer is increased (from 300 mm to 450 mm), has environmental benefits along with the cost-saving offered as recycling of the pavement at a later date is easy as the granular layer is an un-bound layer.

## 4.5 DESIGN FOR GEOGRID-REINFORCED FLEXIBLE PAVEMENT

Through the study, the bituminous layer thickness is reduced. From table 4.2, two cost-efficient pavement sections are chosen (alternative 1 and 2). The rutting and fatigue lives of the cost-efficient pavement composition 1 is found to be higher than the cost-efficient pavement section 2 (table 4.1). Therefore, the chosen bituminous layer thickness and granular layer thickness from the study are 60 mm and 450 mm (225 mm base and 225 mm GSB). A geogrid's primary stabilization mechanism is lateral restraint of the subbase or base materials through a process of interlocking the aggregate and the apertures of the geogrid. The level of lateral restraint that is achieved is a function of the type of geogrid and the quality and gradation of the base or subbase material placed on the geogrid. To maximize performance of the geogrid, a well-graded granular base or subbase material should be selected that is sized appropriately for the aperture size of the geogrid. When aggregate is placed over geogrid, it quickly becomes confined within the apertures and is restrained from punching into the soft subgrade and shoving laterally. This results in a "stiffened" aggregate platform over the geogrid. Very little deformation of the geogrid is needed to achieve the lateral restraint and reinforcement.

The effect of decreasing the thickness of granular layers by using a geogrid reinforcement is studied for an effective subgrade CBR of 5% and design traffic of 2.89 msa.

**Input data:**

Design traffic: 2.89 msa,

Subgrade CBR = 5%

Solution:

i. Design resilient modulus of the compacted subgrade

$M_R = 10 * 5 = 50$ MPa

ii. Thickness of unreinforced granular layers:

Thickness of granular base ($D_2$) = 225 mm,

Thickness of granular sub-base ($D_3$) = 225 mm

Therefore, resilient modulus of granular layer = $0.2 \times (450)^{0.45} \times 50$

= 156.2952 MPa.

Thickness of proposed bituminous layer with VG 40 bitumen with DBM layer having air void of 3 per cent over WMM and GSB mm at reliability of 80 per cent.

**(A) Design calculations of bitumen pavement with geogrid reinforced granular base and subbase layers using LCR of geogrid**

**Reducing thickness of pavement section**

In this case the effect of reinforcement is shown as the reduction in the pavement section thickness.

i. Design Traffic = 2.89 msa
ii. Subgrade CBR = 5 per cent
iii. Reliability = 80 per cent
iv. Resilient Modulus of Subgrade ($M_R$): $M_R$ (MPa) = 10 ×5 = 50 MPa

Resilient modulus of Subbase and Base layers:

Granular sub-base thickness ($M_{R\_GSB}$) = 225 mm

$M_R$ of unreinforced subbase layer = $0.2 \times (225)^{0.45} \times 50$ = 114.415 MPa

= 16594.49 Psi

Granular Base thickness = 225 mm

$M_R$ of unreinforced base layer = $0.2 \times (225)^{0.45} \times 114.415$ = 261.814 MPa

= 37973.101 Psi

Resilient modulus of Bituminous Mixes = 2512 MPa=364335.456 Psi

v. Structural layer coefficient of each layer:

Layer coefficient for bituminous layer ($a_1$) = 0.171 x (ln ($M_R$))-1.784

= 0.171 x (ln (364335.456))-1.784 = 0.405

a) Structural Layer coefficient for base layer shall be taken from the equations given in AASTHO 1993.

Structural layer coefficient for base layer

$a_2 = 0.249 \times (\log_{10} M_{R\_BC}) - 0.977 = 0.249 \times (\log_{10} 37973.101) - 0.977$

= 0.163

b) Structural layer coefficient for subbase layer

$a_3 = 0.227 (\log_{10} M_{R\_SB}) - 0.839 = 0.119$

Therefore,

Layer coefficient for base layer ($a_2$)= 0.163

Layer coefficient for sub base layer ($a_3$) = 0.119

vi. Layer Coefficient Ratio: Layer coefficient for geogrid is taken on the basis on the laboratory tests/filed tests; or it can be provided by the manufacturer.

($LCR_{base}$) for geogrid used in base layer = 1.4

($LCR_{Subbase}$) for geogrid used in sub base layer = 1.61

(B)Modified layer thickness values for reinforced sections by IITPAVE

Thickness of sub base layer = 200 mm

Thickness of base layer = 90 mm

Resilient modulus of reinforced Subbase and Base layers

Granular sub-base thickness = 200 mm

$M_R$ of reinforced subbase layer = $0.2 \times (200)^{0.45} \times 50$ = 108.508 MPa =15737.7833 Psi

Granular Base thickness = 90 mm

$M_R$ of reinforced base layer = $0.2 \times (90)^{0.45} \times 108.508$ = 164.399 MPa

= 23844.196 Psi

Layer coefficient for bituminous layer ($a_1$) = 0.405

c)Structural Layer coefficient for base layer shall be taken from the equations given in AASTHO 1993.

Structural layer coefficient for base layer

$a_2 = 0.249 \times (\log_{10} M_{R\_GB}) - 0.977 = 0.249 \times (\log_{10} 23844.196) - 0.977$

= 0.113

d)Structural layer coefficient for subbase layer

$a_3 = 0.227 (\log_{10} M_{R\_GSB}) - 0.839 = 0.227 \times (\log_{10} 15737.7833) - 0.839$

= 0.114

Therefore,

Modified layer coefficient for base layer ($a_2$') = $LCR_{base} \times a_2$

= 1.4*0.113 = 0.158

Modified layer coefficient for sub-base layer ($a_3$') = $LCR_{Subbase} \times a_3$

= 1.61*0.1137= 0.183

With the improved layer coefficients, improved elastic modulus of respective layers shall be back calculated using below equations.

$a_2' = 0.249 \times (\log M_{R\_GB1}) - 0.977$, $M_{R\_GB1}$ = 249.642 MPa

$a_3' = 0.227 (\log M_{R\_GSB1}) - 0.839$, $M_{R\_GSB1}$ = 219.138 MPa

Using above improved elastic modulus corresponding improved layer coefficients, reinforced layer thickness shall be determined.

Reinforced base layer thickness = 90 mm

Reinforced subbase layer thickness = 200 mm

Surface layer (DBM) =60 mm

Considering design Traffic as 2.89 msa and for 80% reliability,

$$N_R = 4.1656 \times 10^{-08} [1/\varepsilon_v]^{4.5337}$$

$$2{,}897{,}935 = 4.1656 \times 10^{-08} [1/\varepsilon_v]^{4.5337}$$

$$\varepsilon_v = 0.88465 \times 10^{-03} \text{ micro-strain units}$$

$$N_f = 2.21 * 10^{-4} * [1/\varepsilon_t]^{3.89} * [1/M_{Rm}]^{0.854}$$

$$2{,}897{,}935 = 2.21 * 10^{-4} * [1/\varepsilon_t]^{3.89} * [1/2512]^{0.854}$$

$$\varepsilon_t = 0.4493 \times 10^{-03} \text{ micro-strain units}$$

This reinforced pavement section shall be designed as per IRC:37 i.e. section shall be checked for fatigue and rutting failure criterion by inputting this improved elastic modulus into IITPAVE. Obtained vertical strain at subgrade level is $0.8567 \times 10^{-03}$, which is less than the permissible vertical strain $0.88465 \times 10^{-03}$ for 2.89 msa traffic and obtained tensile strain at bottom of bituminous layer is $0.3232 \times 10^{-03}$ is less than permissible tensile strain obtained ie, $0.4493 \times 10^{-03}$ as shown in figure 4.22. Hence the reduced section with geogrid reinforcement in base and subbase layers is acceptable for design traffic 2.89 msa.

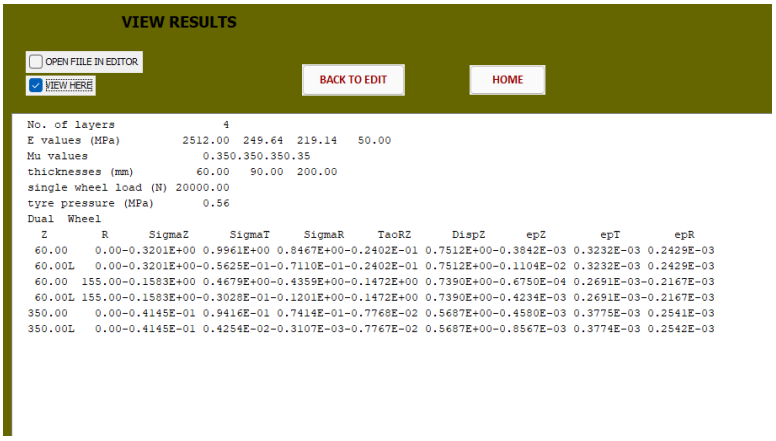


Figure 4. 22 Snapshot of output in IITPAVE (Compressive and Tensile Strains Induced in the Pavement Layers for Reinforced Section)

Table 4.3 gives the overview of the reduced pavement sections designed using the mechanistic-empirical approach, which are cost-efficient and satisfies the performance criteria as per design. The snapshot of L-Graph of the third modified section designed in KENLAYER is presented in figure 4.23.

Table 4.3 Designed reduced pavement sections

| **PAVEMENT SECTION** | **DETAILS OF PAVEMENT SECTIONS** | **THICKNESSES OF PAVEMENT LAYERS** | | | | |
|---|---|---|---|---|---|---|
| | | **DBM** | **BASE** | **GSB** | **COMPACTED SUBGRADE (CBR = 6%)** | **EMBANKMENT (CBR = 3.71)** |
| Conventional | Existing pavement section on the road | 120 | 100 | 200 | _ | _ |
| Modified(1) | Modified pavement section with non-woven polyester geotextile placed at H/4 from the top of compacted subgrade | 90 | 100 | 200 | 500 | _ |
| Modified(2) | Modified pavement section with non-woven polyester geotextile placed at H/4 from the | 60 | 225 | 225 | 500 | _ |

| | | | | | | |
|---|---|---|---|---|---|---|
| | top of compacted subgrade | | | | | |
| Modified(3) | Modified pavement section with non-woven polyester geotextile placed at H/4 from the top of compacted subgrade and geogrid placed in the base layer at the bottom and in the GSB layer at a depth of H/2 to H/3 from top. | 60 | 90 | 200 | 500 | _ |

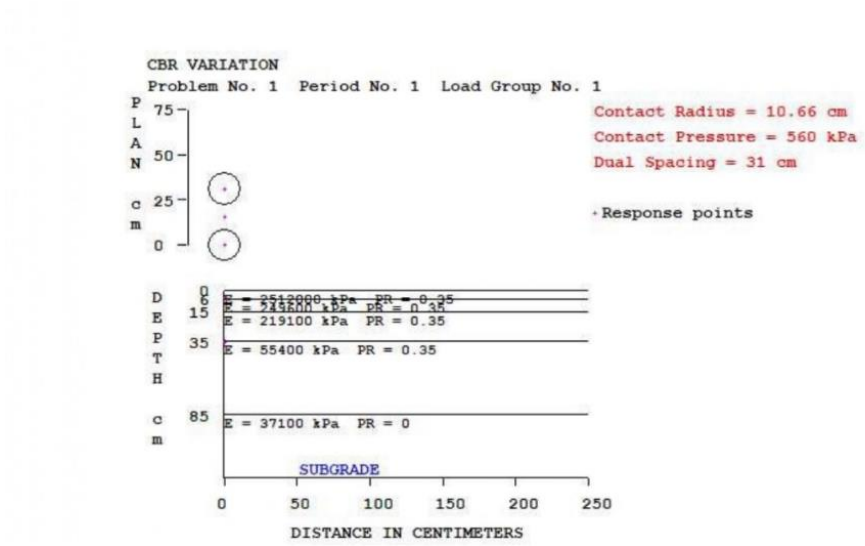


Figure 4. 23 Snapshot of L-graph of a modified pavement section in KENLAYER

# CHAPTER 5

# CONCLUSION

From pavement studies analyzed in this project, it can be concluded that layered elastic analysis is a reasonable approximation of actual pavement responses under both static and dynamic wheel loads. The layered elastic method is suitable to predict pavement responses for different environmental and loading conditions. The utilization of software's like KENPAVE and IITPAVE help in the selection of materials for the pavement and the performance of pavement can be evaluated more accurately. The results are matching well in the linear elastic analysis in both IITPAVE and KENPAVE. The improvement in the performance parameters after using adequate materials in the subgrade like geosynthetics is reflected in the study. When the geotextiles are placed at one-fourth depth from the top, the rutting and fatigue lives increased by 1.2 times compared to the rutting and fatigue lives associated with the geotextiles placed at one-fourth depth from the bottom in almost 90% of cases. The rutting and fatigue lives estimated for subgrades stabilized with synthetic geotextile (non-woven polyester) were found to be about 1.4 times higher than the subgrades stabilized with natural geotextile (coir geotextile). Also, when analysing the submergence of the subgrade layer, the seven-day submerged condition has the critical values for mechanistic parameters for linear-elastic condition. When the subgrade was submerged for 7 days and 14 days, adequate geosynthetics like non-woven polyester had decreased the values of deflection at the bottom of bituminous layer from its conventional condition by 1.01 times and increased the values of rutting and fatigue life from its conventional condition by 5.2 times and had almost brought back the pavement to the 4-day submerged conventional state. The damage ratio of the pavement is found to decrease by about 45%, when subgrade CBR is improved to 6% from 3.71%. The damage ratio associated with the pavement sections designed for effective CBR and improved elastic moduli of pavement layers, were found to be about 45% less than the damage ratio associated with the pavement sections designed for the conventional case. The effect of increasing the subgrade CBR along with an increase in the elastic moduli of subgrade and granular layers had increased the rutting and fatigue lives of even thin bituminous surfaced pavements. The increase was about 3.5 times for rutting life and about 2.1 times for fatigue life from the rutting and fatigue life values estimated for the existing state of pavement in the location. The thickness of the bituminous surface layer is halved and the thickness of the base layer was further reduced by using a geogrid

reinforcement in the base and sub-base layers. Hence, through this study, reduced sections were designed to carry an existing design traffic of 2.89 msa.

# CHAPTER 6

# REFERENCES


1. AASHTO. (2008). Mechanistic-empirical pavement design guide: A manual of practice, Interim Ed. Washington, DC.
2. Abdul Naser Abdul Ghani , Nur Izyan Roslan and Ahmad Hilmy Abdul Hamid., (2016). “Road submergence during flooding and its effect on subgrade strength”. *International Journal of Geomate*, 10(21), 1848-1853.
3. Anna-Katharina Wild, Michael Thomas Marx and Gerhard Eisenbeis., (2009). “A new method to simulate the hydrological state of soil under natural conditions”. *ASCE* , 44(8), 843-851.
4. A.V Hankare , P. B Sankpal , V. M Kumbhar and V. B Patil., (2018). “Estimating flexible pavements flood resilience”. *International journal of advance research and development*, 3(2), 30-34.
5. DSR 2021. Delhi schedule of rates, *CPWD*, New Delhi. https://cpwd.gov.in/Publication/DSR_Vol_2_2021.pdf, Accessed on 25th September 2021.
6. Dr. K.R. Arora, Soil mechanics and foundation engineering (Geotechnical engineering), 7th Ed.
7. https://www.onmanorama.com/news/kerala/2018/08/11/ksrtc-resumes-ac-road-service-26-water-logged-days.html
8. Introduction to pavement design, *handout*, *Civil IIT Bombay*.
9. IRC: 37-2012 and IRC: 37-2018. Guidelines for the design of flexible pavements. The Indian Roads Congress, New Delhi.
10. IRC: SP: 72-2015. Guidelines for the design of flexible pavements for low volume ruralroads. The Indian Roads Congress, New Delhi.
11. IRC SP:59-2019, Guidelines for use of geosynthetics in road pavements and associated works. The Indian Roads Congress, New Delhi.
12. Jayakumar J., Venkatesh J. and Selvarajan, Y., R., (2020). “Expansive Subgrade Strength Improvement using Geogrid and Geotextile Layers”. *IOP Conference Series: Materials Science and Engineering*, 955.

13. Kin-ming Chan & Yuhong Wang., (2020). " Resilient pavement design with consideration of flooding effect caused by climate change", *Transportmetrica A: Transport science*, 16(3), 1136–1155.
14. Lekha, B. M. (2016). Performance Studies on Pavements Using Chemically Stabilized Soils (Doctoral dissertation, National Institute of Technology Karnataka, Surathkal).
15. Louay N. Mohammad, Baoshan Huang, and J. Puppala, and Aron Allen., (2019). "Regression Model for Resilient Modulus of Subgrade Soils". *Transportation Research Record 1687*, 99-1442.
16. Maria Pregnolato., Alistair Ford., Sean M. Wilkinson and Richard J. Dawson., (2017). "The impact of flooding on road transport: A depth- disruption function". *Transport Research Part D: Transport and Environment,* 55, 67-81.
17. Masuda Sultana, Gary Chai, Tim Martin and Sanaul Chowdhury., (2015). "A Study on the Flood Affected Flexible Pavements in Australia". *ICPT 2015.*
18. Masuda Sultana, Gary Chai, Sanaul Chowdhury, Tim Martin, Yuri Anissimov, and Anisur Rahman., (2018). "Rutting and Roughness of Flood-Affected Pavements: Literature Review and Deterioration Models". *Journal of infrastructure systems*, 24(2),1-10.
19. Misbah U. Khan, Mahmoud Mesbah, Luis Ferreira and David J., (2014). "Developing a road deterioration model incorporating flooding." Proc. Transp. Inst. Civ. Eng., 167(5), 322–333.
20. Misbah U. Khan, Mahmoud Mesbah, Luis Ferreira and David J., (2014). "Development of road deterioration models incorporating flooding for optimum maintenance and rehabilitation strategies." Road Transp. Res. J. Aust. N. Z. Res. Pract., 23(1), 3–24.
21. Misbah U. Khan, Mahmoud Mesbah, Luis Ferreira & David J. Williams., (2017). "A case study on pavement performance due to extreme moisture intrusion at untreated layers". *International Journal of Pavement Engineering*, 1029-8436.
22. Misbah U. Khan, Mahmoud Mesbah, Luis Ferreira and David J., (2017). "Estimating pavements flood resilience". *Journal of Transportation Engineering.*, Part B: Pavements, 143(3), 1-8.
23. M. K. Nivedya, Mingjiang Tao, Rajib B. Mallick, Jo Sias Daniel & Jennifer M. Jacobs., (2018). "A framework for the assessment of contribution of base layer

performance towards resilience of flexible pavement to flooding". *International journal of pavement engineering*, 1029-8436.

24. Mohamed Elshaer, Majid Ghayoomi and Jo Sias Danie., (2017). " Impact of subsurface water on structural performance of inundated flexible pavements". *International Journal of Pavement Engineering*, 1029-8436.
25. Mohan, A. N. and Kumar, P. (2020). Analysis of Flexible Pavement using IITPAVE Software and Economic Analysis of the Project using HDM-4 Software. *International Journal for Research in Applied Science and Engineering Technology, 8(5),* 2651-2657.
26. Ogundare D., Familusi O. A. and Olusami J., (2018). "Utilization of Geotextiles for Soil Stabilization". *American Journal of Engineering Research*, 7(1), 224 - 231.
27. Oleiwei G. H., Aodah H. H., Al-obaidy N. K. and Alomari K., (2020). "A Critical Review of Subgrade Soil Reinforced with Geosynthetics", *IOP Confere*nce *Series: Materials Science and Engineering*, 1076.
28. Rind, T. A., Jhatial, A. A., Sandhu, A. R., Bhatti, I. A., and Ahmed, S. (2019). Fatigue and Rutting Analysis of Asphaltic Pavement Using "KENLAYER" Software. *Journal of Applied Engineering Sciences, 9*(2), 177-182.
29. Sachin Kumar, Manish Kumar, Rajesh Kumar, Shubham Singh, Pradeep Kumar and Manish Sharma., (2020). "Design of flexible pavement". *Universe International Journal of Interdisciplinary Research*, 1(2), 2582-6417.
30. Sayed Masoud Mousavi , Majid Ghayoomi , Eshan V. Dave., (2021). " A system dynamics framework for mechanistic analysis of flexible pavement systems under moisture variations", *Transportation Geotechnics, Elsevier*, 2214-3912.
31. Shriram Marathe , Anil Kumar , Avinash., *(2016)."*Investigation on fatigue and durability behaviour of lateritic soil stabilized with cement*", International Journal of Innovative Research In Science*, 5(1), 437-444.
32. Singh M., Trivedi A. and Shukla S. K., (2019). "Strength enhancement of the subgrade soil of unpaved road with geosynthetic reinforcement layers". *Transportation Geotechnics,*19, 54-60.
33. S.K Khanna, C.E.G. Justo, A.Veeraragavan, *Highway engineering*, revised 10th Ed.

34. Sudam P. A., Padmavathi M., Ravikumar K. and Nagaraju M., (2019). ”An Experimental Study on CBR of Expansive Soil Subgrades using Geotextiles”. *International Journal of Civil and Structural Engineering Research*, 7(1), 119-128.
35. Visvanathan, A., Velayudhan, S., and Mathew, S. (2020). Field evaluation of coir geotextile reinforced subgrade for low volume pavements. *Journal of Natural Fibers*, 1-13.
36. Yuhong Wang, Yu Huang, Wit Rattanachot, K.K. (Woody) Lau and Suchatvee Suwansawas., (2014). " Improvement of Pavement Design and Management for More Frequent Flooding by Climate Change'. *Advances in Structural Engineering*, 18(4), 487- 486.